

University of Windsor

## Scholarship at UWindsor

---

Electronic Theses and Dissertations

Theses, Dissertations, and Major Papers

---

2-28-2024

# Greenhouse Cucumber Detection and Characterization for Harvesting Framework Implementation

Shahryar Ghorbanirezaei  
*University of Windsor*

Follow this and additional works at: <https://scholar.uwindsor.ca/etd>

---

### Recommended Citation

Ghorbanirezaei, Shahryar, "Greenhouse Cucumber Detection and Characterization for Harvesting Framework Implementation" (2024). *Electronic Theses and Dissertations*. 9447.  
<https://scholar.uwindsor.ca/etd/9447>

This online database contains the full-text of PhD dissertations and Masters' theses of University of Windsor students from 1954 forward. These documents are made available for personal study and research purposes only, in accordance with the Canadian Copyright Act and the Creative Commons license—CC BY-NC-ND (Attribution, Non-Commercial, No Derivative Works). Under this license, works must always be attributed to the copyright holder (original author), cannot be used for any commercial purposes, and may not be altered. Any other use would require the permission of the copyright holder. Students may inquire about withdrawing their dissertation and/or thesis from this database. For additional inquiries, please contact the repository administrator via email ([scholarship@uwindsor.ca](mailto:scholarship@uwindsor.ca)) or by telephone at 519-253-3000ext. 3208.

**Greenhouse Cucumber Detection and Characterization for Harvesting Framework  
Implementation**

By

**Shahryar Ghorbanirezaei**

A Thesis  
Submitted to the Faculty of Graduate Studies  
through the Department of Mechanical, Automotive and Materials Engineering  
in Partial Fulfillment of the Requirements for  
the Degree of Master of Applied Science  
at the University of Windsor

Windsor, Ontario, Canada

2024

© 2024 Shahryar Ghorbanirezaei

**Greenhouse Cucumber Detection and Characterization for Harvesting Framework  
Implementation**

By

**Shahryar Ghorbanirezaei**

APPROVED BY:

---

M. Hassanzadeh  
Department of Electrical and Computer Engineering

---

J. Johrendt  
Department of Mechanical, Automotive and Materials Engineering

---

J. Urbanic, Advisor  
Department of Mechanical, Automotive and Materials Engineering

February 16, 2024

## DECLARATION OF ORIGINALITY

I hereby certify that I am the sole author of this thesis and that no part of this thesis has been published or submitted for publication.

I certify that, to the best of my knowledge, my thesis does not infringe upon anyone's copyright nor violate any proprietary rights and that any ideas, techniques, quotations, or any other material from the work of other people included in my thesis, published or otherwise, are fully acknowledged in accordance with the standard referencing practices. Furthermore, to the extent that I have included copyrighted material that surpasses the bounds of fair dealing within the meaning of the Canada Copyright Act, I certify that I have obtained a written permission from the copyright owner(s) to include such material(s) in my thesis and have included copies of such copyright clearances to my appendix.

I declare that this is a true copy of my thesis, including any final revisions, as approved by my thesis committee and the Graduate Studies office, and that this thesis has not been submitted for a higher degree to any other University or Institution.

## ABSTRACT

Cucumbers constitute a significant portion of greenhouse vegetables cultivated in southern Ontario. The human labour shortage and potential injuries associated with manual labour in cucumber harvesting highlight the need to explore automation as a viable solution. The proposed automated system in this study comprises two key components: an image processing unit and a cutting robotic arm. The image processing phase involves the identification of cucumbers using six models using shape and colour features. Four models are successfully employed in YOLOv8, yielding results in the form of bounding boxes and keypoints, with no false positives. Near-real-time cucumber detection is also achieved using YOLO. One model has been successfully tested in RoboFlow. Finally, one new model is being initially investigated for the direct management of raw RGB-XYZ data in Python. About harvesting unit, a robotic arm equipped with a cutting tool is programmed to move to specific positions and perform cutting tasks. To enable this functionality, a 3D camera and cutter are integrated into the TCP of a UR3e robot. The 3D camera installed on TCP of the robot can move at angles and positions to capture cucumbers hidden from view. Additionally, analyses of cucumber geometry and force are carried out to improve the understanding of cucumber properties. Finally, initial cost and OEE analyses are conducted to assess the potential improvement resulting from transitioning from manual harvesting to automation.

*Keywords: Image Detection; YOLO; Robotic Arm; Shape and Colour Features; Cucumber Characteristics; Force Analysis; Geometry Analysis; 3D Camera.*

# TABLE OF CONTENTS

DECLARATION OF ORIGINALITY .....	iii
ABSTRACT.....	iv
LIST OF TABLES .....	viii
LIST OF FIGURES .....	ix
NOMENCLATURE .....	xi
1. INTRODUCTION.....	1
1.1. Greenhouse Statistics in Ontario.....	1
1.2. Traditional manual greenhouse harvesting .....	3
1.3. Automation as a substitute for traditional harvesting .....	4
1.4. Problem definition and functional requirements.....	5
1.4.1. Problem space .....	5
1.4.2. Research Statement.....	6
1.4.3. Functional requirements and limitations.....	6
1.5. Research goals .....	7
2. LITERATURE REVIEW .....	8
2.1. Statistical analysis of literature documents.....	8
2.2. Literature review and matrix.....	9
2.3. Research gap.....	16
3. METHODOLOGY AND TEST SETUP.....	17
3.1. Proposed model.....	17
3.2. Flow diagrams of the proposed model.....	17
3.2.1. Process and event flow diagrams .....	17
3.2.2. Data flow diagram.....	18
3.3. Experimental tools and equipment.....	19
3.4. Software tools .....	19
3.5. Metrics in image processing evaluation.....	21
3.6. Artificial greenhouse.....	21

3.7.	Camera setup and calibration .....	22
3.8.	Camera and cutter movement control using UR3e .....	23
3.9.	Object detection using popular pretrained models.....	24
3.10.	Cucumber bounding box detection using two models in YOLOv8 .....	25
3.11.	Cucumber keypoints detection using two models in YOLOv8.....	26
3.12.	Cucumber bounding box detection using one model in RoboFlow .....	26
3.13.	Cucumber shape detection using raw RGB-XYZ data .....	26
3.14.	Communication between image processing and robotic arm.....	27
3.15.	Force analysis using pressure sensors .....	28
3.16.	Geometry analysis with MATLAB.....	28
4.	RESULTS AND DISCUSSION.....	30
4.1.	Cucumber bounding box and keypoints detections using YOLOv8.....	30
4.1.1.	Bounding box.....	30
4.1.2.	Near-real-time cucumber detection using YOLON .....	33
4.1.3.	Cucumber keypoints detection with YOLOv8 .....	35
4.2.	Robotic arm movement.....	37
4.3.	Geometry MATLAB analysis results .....	40
4.4.	Managing RGB-XYZ data in Python.....	47
4.5.	Force analysis.....	48
4.6.	Cost analysis .....	53
4.7.	OEE analysis .....	56
4.8.	Summary .....	57
5.	CONCLUSION AND FUTURE .....	59
	REFERENCES .....	60
	APPENDICES .....	63
	APPENDIX A. UR3e specifications.....	63
	APPENDIX B. D435if: Intel RealSense software and specifications .....	64
	APPENDIX C. Camera setup and calibration .....	66
	APPENDIX D. Managing RGB-XYZ data in Python.....	69
	APPENDIX E. Client interfaces .....	70
	APPENDIX F. Container.....	72
	APPENDIX G. Geometry analysis .....	73

APPENDIX H. Detailed data collection plan .....	78
Appendix I. Boundary detection using ImageJ and Fiji.....	98
Appendix J. Cucumber bounding box detection using Roboflow platform.....	100
VITA AUCTORIS .....	101



## LIST OF TABLES

Table 2-1. Literature review matrix .....	15
Table 3-1. Comparison between three of popular pretrained models.....	24
Table 4-1. Summary of metrics for cucumber bounding box detection.....	33
Table 4-2. Summary of metrics for cucumber keypoints detection .....	37
Table 4-3. RGBs' intervals for type 1 plant's components.....	48
Table 4-4. RGBs' intervals for type 2 plant's components.....	48
Table 4-5. Cost analysis results in manual cucumber harvesting .....	54
Table 4-6. Cost analysis results in automation of cucumber harvesting .....	55

## LIST OF FIGURES

Figure 1-1. 2021 statistics on Canadian greenhouses [1-2] .....	3
Figure 1-2. The problem space of this research shown in seven blocks .....	6
Figure 1-3. Functional requirements for automating cucumber harvesting processes in greenhouses.....	7
Figure 2-1. Statistical analysis of the literature using Bibliometrix, Biblioshiny, and RStudio indicate a trend.....	8
Figure 2-2. Utilizing new keywords to narrow down the search results and identify the most pertinent documents. ....	9
Figure 2-3. Thematic map of the literature and the position of the current research .....	9
Figure 2-4. A dual arm harvester developed by Yoshida et al with an accuracy of 95% [13] .....	13
Figure 2-5. Pose estimation method proposed by Eizentals et al [15] .....	13
Figure 2-6. Device configuration for automated yield monitoring system for detection of location of target plants [16] .....	14
Figure 2-7. Gripper designed for harvesting apples using a robotic arm [17] .....	14
Figure 3-1. Overview of the proposed model of the automated cucumber harvester .....	17
Figure 3-2. The process and event flow diagram of the proposed automated harvester.....	18
Figure 3-3. Data flow of the proposed model .....	18
Figure 3-4. Sample CAD files for the artificial: a. peppers, b. apples, and c. cucumbers before 3D printing.....	21
Figure 3-5. a. 3D printed peppers, cucumbers, and apples, and b. The post-processing ....	22
Figure 3-6. In-house artificial setup.....	22
Figure 3-7. The dynamic calibration print target should be placed in 16 different positions for camera calibration .....	23
Figure 3-8. Camera movement at different angles and directions .....	23
Figure 3-9. An example of labeled cucumbers using CVAT.....	26
Figure 3-10. Left: visualization of target RGB values for cucumber, vine, and leaf (each square assumed to be a pixel). Middle: false positives and false negatives pixels. Right: after removing false positives and retaining false negatives, a complete cucumber shape is maintained, while all leaves and vines effectively filtered out .....	27
Figure 3-11. a. Experimental setup to find the peak forces that each cucumber can tolerate and a damage cucumber after applying force, b. Damaged cucumber after applying force on its surface .....	28
Figure 4-1. YOLOL: two images with their detected cucumbers and their confidences....	31
Figure 4-2. F1-confidence curve in YOLOL .....	31
Figure 4-3. YOLON: two images with related detection confidences.....	32
Figure 4-4. F1 and confidence relationship in YOLON .....	32
Figure 4-5 (a) through (e). Near-real-time cucumber detection in a video from real greenhouse using YOLOL .....	35
Figure 4-6. Detecting the cucumber pose and identifying keypoints to determine the position of the stem end in YOLOL (a), and YOLOX (b).....	36
Figure 4-7. F1 and confidence graph in pose-YOLOL .....	36

Figure 4-8. F1 and confidence relationship in pose-YOLOX.....	37
Figure 4-9. a through e. Robot trajectory to harvest detected cucumbers based on received position data.....	39
Figure 4-10. Final flowchart of the system including input/output, decision-making and harvesting.....	40
Figure 4-11. the experimental arrangement for the initial cucumber sample (a), and the resulting image displayed in the RealSense software (b).....	40
Figure 4-12 MATLAB curve fittings of orders 2 (a) and 3 (b) for first cucumber sample.....	42
Figure 4-13 The experimental setup for the second cucumber sample (a) and the resultant image exhibited in the RealSense software (b).....	42
Figure 4-14 MATLAB curve fittings of degrees 2 (a) and 3 (b) for the second cucumber sample.....	43
Figure 4-15 The experimental arrangement for the third cucumber sample (a) and the resulting image displayed in the RealSense software (b).....	43
Figure 4-16. MATLAB curve fits of orders 2 (a) and 3 (b) for the third cucumber sample. ....	44
Figure 4-17 The experimental setup for the fourth cucumber sample (a), along with the resultant image showcased in the RealSense software (b).....	45
Figure 4-18 MATLAB curve fittings with orders 2 (a) and 3 (b) for the fourth cucumber sample.....	46
Figure 4-19 The experimental configuration for the fifth cucumber sample (a), accompanied by the resulting image displayed in the RealSense software (b).....	46
Figure 4-20. MATLAB curve fittings of degrees 2 (a) and 3 (b) for the fifth cucumber sample.....	47
Figure 4-21. Samples for experimental test on peak tolerable force.....	49
Figure 4-22. a. The direction of applying force, and b. The effect of colour on peak load	50
Figure 4-23. a. The direction of applying force, and b. The effect of curvature on peak axial load.....	51
Figure 4-24. a. The direction of applying force, and b. The effect of diameter on peak load.....	52
Figure 4-25. a. The direction of applying force, and b. The effect of angle on peak load..	52
Figure 4-26. a. The direction of applying force, and b. Effect of cucumber length on peak load.....	53

## NOMENCLATURE

3D camera	A camera gives XYZ-RGB data of each pixel
3D printing	Material deposition layer by layer in 3 axes. Additive manufacturing
3D shape data	x, y, z data
Annotation	Adding labels or mark to images
Augmentation	Adding various transformations, such as rotation and scaling to an image
Bounding box	A rectangle drawn around a target object
Classification	Assign categories to different images
Collaborative robot	Robots that work human
Colour threshold	Setting and filtering special pixels to isolate a target
CVAT	Computer Vision Annotation Tool for annotating images
Depth data	Data related to the distance of camera to a pixel (z)
Edge detection	Finding the edges or borders of an object
Feature extraction	Finding special patterns in an image
Fiji	An open access software for image processing
HSV	Hue, Saturation, Value
Image preprocessing	Some step done on a raw image before doing more processes
IMU	Inertial Measurement Unit
Intel RealSense Calibration Print Target	A page with special grid sizes that should be printed for camera calibration. It is provided by Intel
Intel's Dynamic Calibrator software	A software developed by Intel for 3D camera calibration
Keypoints	Some points by which a pose will be detected
Peak tolerable force	Maximum force that cucumber can tolerate before bruising
Pressure sensors	Sensors that convert mechanical stimuli into electrical pulses.
R-CNN	Region-based Convolutional Neural Network
RGB parameters	Red, Green, Blue values of a pixel
RoboFlow	A platform for object detection
RPN	Region Proposal Network
Segmentation	Defining an image to different meaningful regions
SSD	Single Shot Multibox Detector
Super pixel blocks	Mixing some pixels together
TBD	To Be Determined
TCP	Tool Center Point

Teach pendant	A displaying device for manually control a robot motion
UR3e robot	Universal Robots 3e
WIDACS	Wireless Data ACquisition System
YOLO	You Only Look Once; a pretrained object detection algorithm
YOLOL	YOLO Large model
YOLON	YOLO Nano model
YOLOX	YOLO X-large model

## 1. INTRODUCTION

Cucumbers are extensively grown and economically significant crops utilized in both fresh consumption and various food preparations. The cultivation process commonly involves a three-crop system per year, although variations exist with some smaller greenhouses adopting a two-crop system and larger ones employing a four-crop approach. Typically, cucumber plants begin producing cucumbers within 2-3 weeks after transplantation and continue to yield for a period ranging from 60 to 150 days [1].

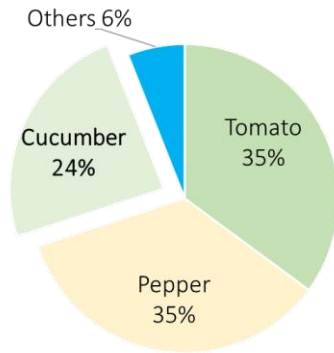
The manual method of cucumber harvesting is labour-intensive, inconsistent, physically damaging on pickers, and time-consuming. The study explores automated harvesting as a substitute, aiming to address labour shortages and health concerns.

This chapter outlines greenhouse statistics in Ontario and Canada, the difference between automation and manual harvesting, the functional requirements for automating greenhouse harvesting and identifies the problem space, focusing on replicating manual cucumber harvesting using robotics. The study aims to design a semi-functional automated cucumber harvester, incorporating cucumber detection through image processing and harvesting with a robotic arm. Specific goals include detecting cucumbers, executing cutting arm trajectories, and collecting data for future modeling.

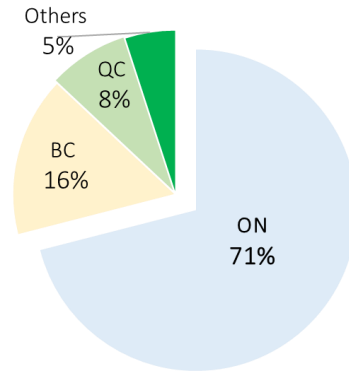
### *1.1.Greenhouse Statistics in Ontario*

Windsor Essex boasts one of the highest greenhouse densities globally, second only to the Netherlands. Canada stands as the fourth-largest cucumber exporter in the world. Figure 1-1.a illustrates the distribution of greenhouse produce in Canada for the year 2021. Given that cucumbers represent a significant greenhouse crop, they constitute the primary focus of this study [2]. Approximately 70 growers in Southern Ontario collectively yield an annual cucumber production of 400 million pounds. Figure 1-1.b indicates that 71% of all greenhouses in Canada are situated in Ontario. Examining Figures 1-1.c and 1-1.d, the 2021 statistics reveal that cucumber cultivation accounts for 237,000 metric tons, with Ontario contributing 321 greenhouses out of a total of 892 across Canada. Interestingly, despite housing only 36% of the total number of greenhouses, Ontario manages to produce 71% of the greenhouse products, underscoring either the presence of larger greenhouses or

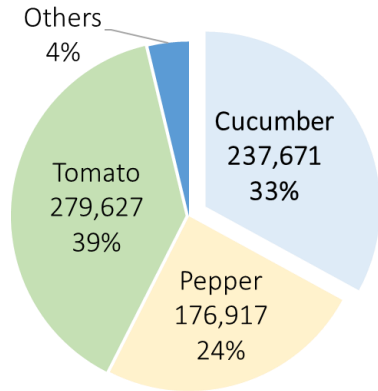
more fertile soil in the province. Furthermore, the farm gate value of greenhouse vegetables for 2021 by province are depicted in Figures 1-1.e and 1-1.f. Ontario emerges as the leader in this regard, with cucumbers ranking second only to peppers, as indicated in Figure 1-1.g. Notably, labour costs account for a significant portion, with 29% of total expenses allocated to human labour. This translates to an expenditure of CAD 27 million for manual labour associated with cucumber harvesting.



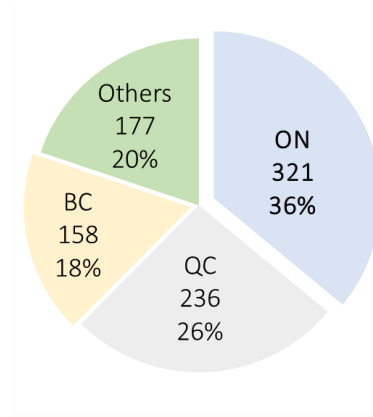
a. Greenhouse distribution by harvested area in Canada



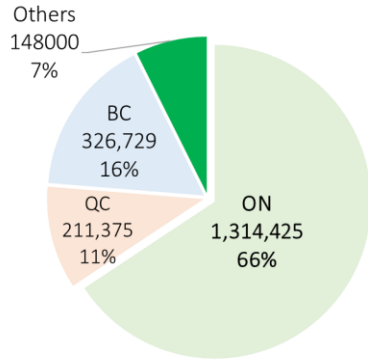
b. Provincial greenhouse distribution by harvested area in Canada



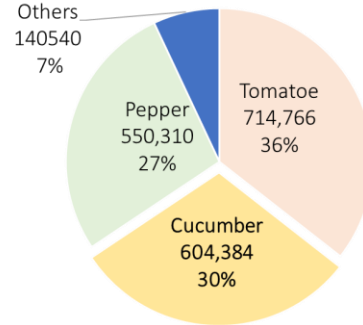
c. Distribution of greenhouse production volumes (in metric tons) in Canada



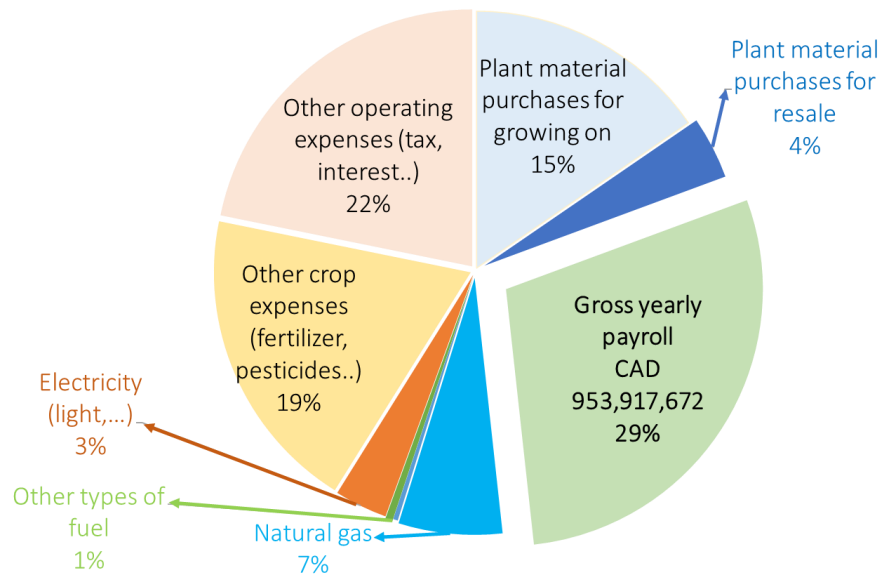
d. Distribution of commercial greenhouses in Canada (total 892 greenhouses)



e. Provincial farm gate value of greenhouse vegetables (in thousands of CAD), calculated as the market value minus selling costs



f. Farm gate value of greenhouse vegetables, measured in thousands of CAD, categorized by each commodity



g. Expenses distribution

Figure 1-1. 2021 statistics on Canadian greenhouses [1-2]

### 1.2. Traditional manual greenhouse harvesting

The practice of manually harvesting cucumbers is referred to as the traditional method of cucumber harvesting. When any form of automation, from planting to harvesting and sorting, is employed in farming operations, it is considered non-traditional cucumber farming. Traditional cucumber cultivation comes with certain drawbacks, which are outlined below.



Harvesting heavily depends on human labour. All farming stages are manual and carried out by workers. In 2021, approximately 5,000 workers are employed in Canadian cucumber greenhouses, encompassing both permanent and seasonal labour. Particularly during the COVID-19 pandemic, labour shortages posed challenges for greenhouse operations.

Processes in traditional greenhouses are not consistently executed. The quality, speed, and efficiency of harvesting heavily rely on the workers' skills, physical strength, and pace. This reliance on human factors introduces inconsistency into the process, leading to unpredictable outcomes. Harvesting quality can vary from season to season and among different farms. Furthermore, the inconsistency in harvesting quality also increases the likelihood of cucumbers being damaged, with the extent of damage depending on each worker.

Traditional harvesting can cause harm to workers. It requires specific body postures that are not in line with normal body alignment, resulting in potential damage to their wrists, necks, backs, and hands [3].

Under standard conditions, it is assumed that each worker can harvest approximately 80-100 small cucumbers per hour. However, factors such as the presence of cucumbers on all plants, the occurrence of diseases, and damaged cucumbers are considered normal. Workers typically do not work during the night or on holidays. In contrast, robots can operate continuously, seven days a week, 24 hours a day (7/24). This is particularly advantageous because the cucumber harvesting window is short, and human workers are limited in the number of hours they can work each week. Consequently, timely harvesting can be a challenge.

### ***1.3.Automation as a substitute for traditional harvesting***

Advancements in robotics and image processing have sparked a substantial transformation in the farming sector, automating tasks previously performed manually. This research tackles critical challenges, notably labour shortages and health concerns, with a specific emphasis on the harvesting process. The primary goals include minimizing cucumber damage, enhancing overall efficiency, and accelerating the harvesting speed.

This approach is crafted for scalability, accommodating both small and large farms. The primary challenges centre on achieving successful detection and precise cutting to prevent damage to both the plants and cucumbers.

#### ***1.4.Problem definition and functional requirements***

The primary focus of this study lies in addressing the challenge of replicating the manual harvesting of cucumbers. The objective is to incorporate this principle into a robotic arm. Similar to humans, the initial requirement for the robot is a visual perception, achieved through a camera functioning as the "eye," while an image processing algorithm serves as its "brain."

##### ***1.4.1. Problem space***

The study is guided by a specific problem space, as illustrated in Figure 1-2. Each space is presented in its corresponding section to facilitate a visual understanding of the problem space. All needed components should be identified and arranged in the proposed device. Particularly crucial is the determination of the camera and cutter placement on the robot. Additionally, the image processing unit must possess the capability to detect cucumbers and pinpoint the stem end for harvesting. This positional data is then transmitted to a robotic arm through an interface. The robot navigates to the designated position with precision, ensuring it avoids unpredicted accidental contact with the plant. Further research on cucumber characteristics, including its geometry and peak tolerable force, is helpful for comprehensive understanding and effective implementation.

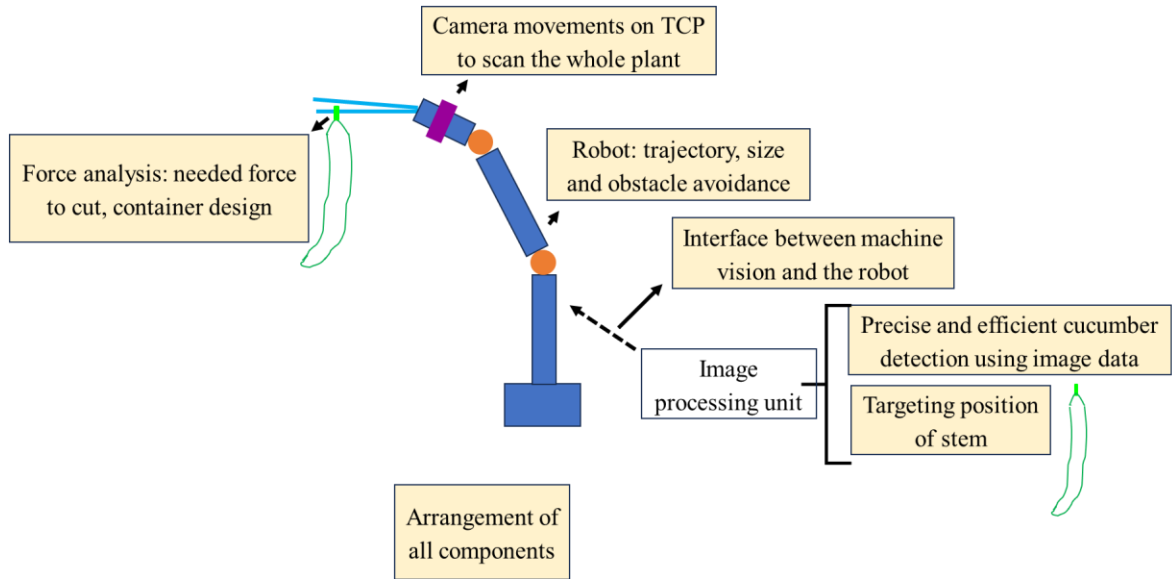


Figure 1-2. The problem space of this research shown in seven blocks

#### 1.4.2. Research Statement

This study aims to apply various cucumber detection algorithms and a robotic arm to detect and harvest greenhouse cucumbers. The methodology involves the utilization of a 3D camera and programming a cutting robotic arm. Additionally, considerations extend to characterize cucumbers by doing force and geometry analysis, along with a preliminary study on managing RGB-XYZ data generated by a 3D camera for shape detection. Establishing a framework for real-time detection considering the dynamic conditions of cucumber greenhouse and its environment is also considered for future studies.

#### 1.4.3. Functional requirements and limitations

The functional requirements, briefly depicted in Figure 1-3, commence with cucumber detection as the initial task. The system is designed to do near-real-time detection. Selection of cucumbers for harvesting is based on specific criteria, requiring a decision-making process. The robot should prevent unpredicted accidents with the plant's components. However, some gentle contact with the plant is unavoidable during harvesting.

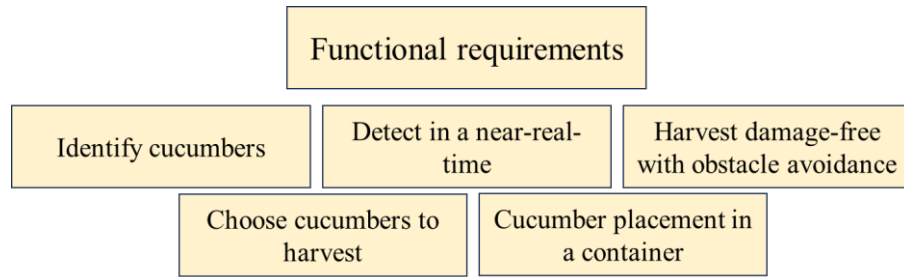


*Figure 1-3. Functional requirements for automating cucumber harvesting processes in greenhouses*

Assigning a task currently performed by a skilled smart human to a robot presents inherent constraints. Some limitations need to be considered, such as “achieving a comprehensive prediction of all dynamic conditions, such as lighting variations that impact detection and harvesting accuracy, may not be feasible, and needs to be an ongoing area of research.”

### ***1.5. Research goals***

Research goals are as follows.

The overarching objective of this research is to design and develop an automated cucumber harvester capable of cucumber and stem end detection and subsequent harvesting using a robot. The specific sub-goals are as follows.

- Detect cucumbers in artificial greenhouses using multiple algorithms.
- Program a cutting robotic arm to harvest detected cucumbers.
- Analyze peak tolerable force and geometry of cucumber, cucumber appearance, and greenhouse environment for future modeling.
- Manage raw data of 3D camera (RGB-XYZ): a preliminary study designed to be adaptable for various types of produces.

Chapter 2 is the literature review, leading to the identification of the research gap. Chapter 3 outlines the methodology and test setup, detailing how the identified gap will be addressed. In chapter 4, the results pertaining to the finalized methodology are presented and discussed. Chapter 5 encapsulates the research's conclusions and outlines directions for future work.

## 2. LITERATURE REVIEW

This section comprises a literature review of previous research. Initially, an examination of various automated harvesters is conducted. Subsequently, the chapter outlines several algorithms proposed in the literature, categorized based on distinct recognition criteria, presented in a matrix format summarizing key points. The final sections of this chapter delve into the research gap within the identified problem space.

### *2.1. Statistical analysis of literature documents*

In the field of automated agricultural robots, numerous research studies have been conducted. Many of these studies tend to focus on specific aspects or components of a fully automated system. Some concentrate on the detection of produce, while others propose innovative gripper designs. Some delve into the trajectory and efficiency of robotic arms, some explore autonomous functionalities, and others investigate mechanical alternatives to improve harvesting.

Bibliometrix, Biblioshiny, and RStudio are chosen for the analysis of trends and available references related to keywords of this research: "agricultural," "image processing," and "automation" in Scopus. Figure 2-1 displays the results of this statistical analysis. The analysis shows that there is a good annual growth rate (6.74%) in this topic.



*Figure 2-1. Statistical analysis of the literature using Bibliometrix, Biblioshiny, and RStudio indicate a trend*

To narrow down the search and reduce the number of documents to a more manageable level and target the specific research challenges, the keywords are adjusted to add "harvester". The statistical analysis is shown in Figure 2-2. As shown in this Figure there

are 17 documents available with the mentioned keywords, which shows a need of research in this domain.

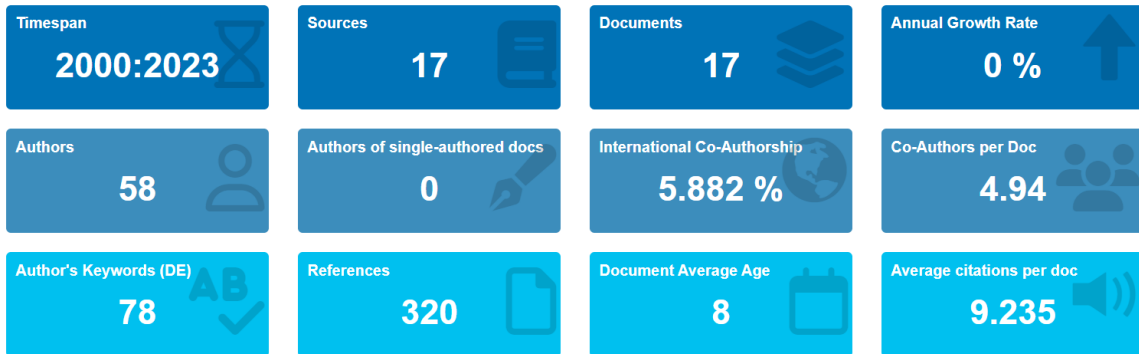


Figure 2-2. Utilizing new keywords to narrow down the search results and identify the most pertinent documents.

The thematic map of the mentioned keywords is also depicted in Figure 2-3. Based on this graph, the current study aligns with the "motor themes" section due to its high relevance to the field and its status as a novel technological advancement. Thus, this research has a distinctive contribution in greenhouse harvesting.

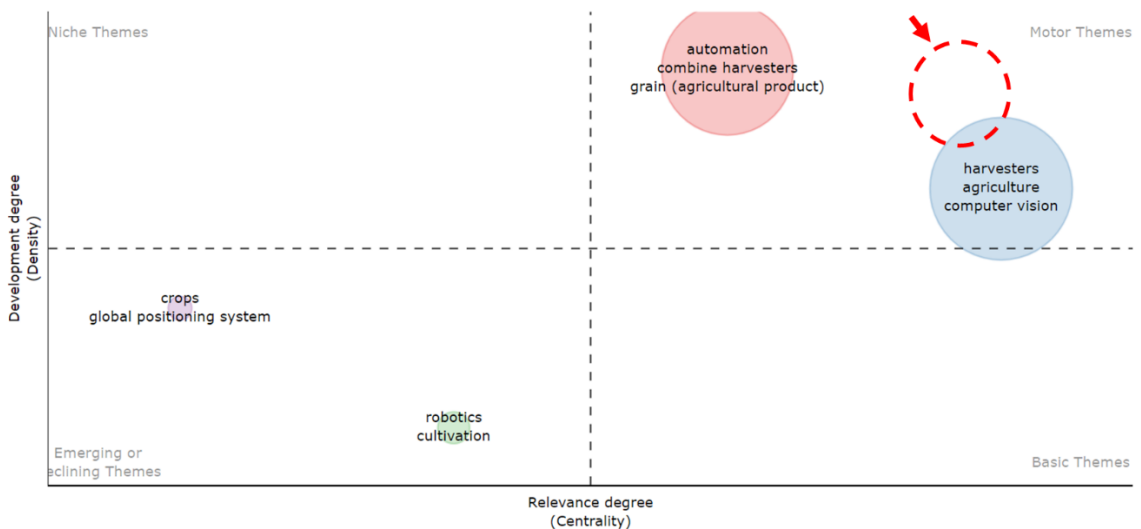


Figure 2-3. Thematic map of the literature and the position of the current research

## 2.2.Literature review and matrix

Jing et al. (2021) studied apples' detection with 1036 images as their dataset [4]. Their algorithm incorporates bounding box detection based on colour information and identifies contours that most accurately represent the shape of the apples. They used contours and RGB as their recognition features. While their model demonstrated a high level of accuracy

(95.66%) and incorporated both RGB and shape data to mitigate reliance solely on RGB information, the study did not delve into the examination of harvesting post-detection. Their model's dependence on the specific dataset used confined its applicability to only the studied apples.

Zheng et al. (2022) conducted a study involving cucumber, eggplant, tomato, and pepper recognition using shape and RGB features [5]. Their dataset comprised 1600 samples, and their model achieved an accuracy range of 80% to 100%. They employed a RealSense D415 camera for data acquisition, which involved a multi-step process. First, they acquired colour images and depth maps, aligning them for subsequent analysis. Then, they employed keypoint detection, utilizing the keypoint RCNN provided by Detectron2, for size estimation. Additionally, they proposed a zoom-in technique to magnify the targets (cucumber, eggplant, tomato, and pepper), enhancing detection accuracy. Finally, they calculated the length and diameter of the recognized objects using 3D space and focal length measurements. While the study covered cucumbers, eggplants, tomatoes and peppers, the accuracy of size estimation and keypoints detection remained inadequate, indicating a need for further investigation. The research did not emphasize the aspects of harvesting and data collection in a greenhouse environment, however.

Gené-Mola et al. (2019) conducted research on Fuji apples, employing recognition features including backscatter signal, RGB, and depth [6]. Their dataset consisted of 967 samples, and their model achieved an impressive accuracy rate of 94.8%. They utilized a Microsoft Kinect sensor for data acquisition and followed a comprehensive methodology. The data preparation process is composed of several steps, including dataset preparation, registration to create a 5-channel multi-modal image combining RGB and depth (RGB-DS), and annotation. In the experimental phase, they employed a Faster R-CNN object detection network, focusing on multi-modals and regions of interest (ROIs) using RPN (Region Proposal Network) for ROI classification. Furthermore, they optimized anchors, specifically bounding boxes, and conducted extensive training to refine their models. Nevertheless, their multiple models significantly relied on colour information, and their study exclusively focused on apple detection without addressing the harvesting aspect.

Kheiralipour et al. (2017) conducted a study on cucumber shapes [7]. They utilize PC1438 and Canon cameras for image acquisition and employed a multi-step methodology. The process involved image preparation, including extracting the blue channel, among other adjustments. Additionally, they extracted both common features like diameter and introduced novel shape features such as centroid non-homogeneity. The final step of their methodology is classification using an artificial neural network (ANN). While they conducted an extensive study on geometry analysis with appropriate metrics, it's noteworthy that their categorization was limited to certain cucumbers, and the study did not include the automation of the process through harvesting.

Rabby et al. (2018) conducted research focused on the detection of oranges and apples utilizing shape and RGB recognition features [8]. However, specific details regarding the number of samples and the best accuracy achieved are not provided. Their approach involved the application of a modified Canny edge detection algorithm. This algorithm underwent several stages, including the computation of horizontal and vertical gradients and their angular directions, identification of candidate points, thresholding, edge connection, and removal of weak edges. Additionally, they employed preprocessing, segmentation, feature extraction encompassing intensity and size, as well as testing, training, and matching procedures in their image processing methodology. While their focus encompasses apples and oranges with varying colours, it's notable that they did not investigate a fully automated harvester.

Liu et al. (2019) conducted research focused on the detection of apples using RGB and shape recognition features [9]. Their dataset comprised 1844 images, achieving an accuracy ranging from 85% to 95.12%. They utilized a Canon IXUS 275HS camera for image acquisition. The key steps in their algorithm included the segmentation of super pixel blocks using Simple Linear Iterative Clustering (SLIC). Subsequently, they extracted colour vectors and trained an SVM classifier. In addition, they worked with rectangular blocks, extracting HOG vectors and again training an SVM classifier. For new images, their approach involved processing super pixel blocks, extracting colour vectors, identifying candidate regions, extracting HOG vectors, and finally detecting the cucumber. However, they did not study detection and harvesting together.



Tu et al. (2020) conducted research focused on counting passion fruits, utilizing both RGB and depth recognition features [10]. Their dataset comprised 2275 samples, and their model achieved an impressive accuracy of 96.2%. They employed a Microsoft Kinect camera for data acquisition. The key steps in their algorithm included RGB data augmentation and a detector based on MS-FRCNN. This process is repeated for depth data. Subsequently, they fused the results from both steps using a linear probability operation to achieve RGB-D detection for passion fruit. They employed multiple models; however, they did not conduct a comprehensive analysis of the passion fruit's geometry nor determine the peak load it can tolerate before bruising. This gap in analysis stems from their exclusion of a complete device in their study.

Iskandar et al. (2022) undertook a study concerning Melinjo fruit detection using both RGB and HSV recognition features [11]. Their dataset consisted of 1,003 samples, achieving an impressive accuracy rate of 98.0%. Their methodology included Google Collaboratory Design and manipulation of RGB and HSV data. This process involved masking for black and white conversion to facilitate background removal. Further steps encompassed the classification of Melinjo into ripe and raw categories based on HSV values. However, they omitted the consideration of the harvesting process, and their model depends on specific dataset and thus is not expandable to other produce.

There have been relatively few instances where comprehensive research has been conducted on fully automated harvesters. One notable example is the root trimmer proposed by McGuinness et al. [12]. This machine is capable of handling lifting, soil removal, root trimming, and sorting of various materials. During its implementation, each subprocess of a field factory is tested and verified on the ground.

Another significant development is the robot with dual arms introduced by Yoshida et al., shown in Figure 2-4 [13]. This robot is equipped with an RGB-D camera, two robotic arms, and two end effectors. It achieved an impressive 95% accuracy rate in produce detection, with a processing speed of 20 seconds per produce.

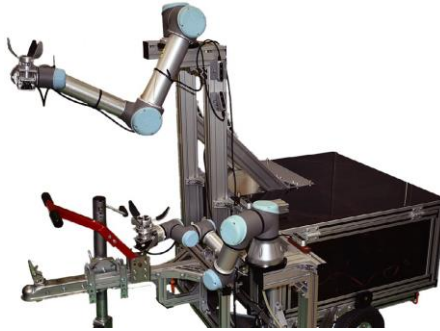


*Figure 2-4. A dual arm harvester developed by Yoshida et al with an accuracy of 95% [13]*

Theoretical aspects of automated harvesting have been explored by Shaprov et al. [14]. Their work involved modeling the system and determining optimal forces to prevent crop damage. However, they solely focused on the theoretical aspects of the harvester.

Eizentals et al. conducted research on the pose estimation of peppers, utilizing a laser range finder, as depicted in Figure 2-5. Their system demonstrated an accuracy rate exceeding 75%, and they tested it in a real farm [15]. They partly considered and analyzed some geometry aspects of peppers. However, the maximum accuracy of their model, which was 77.6%, is insufficient for practical use in real-world scenarios.

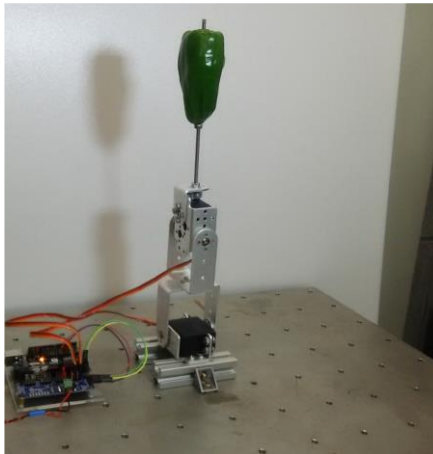


*Figure 2-5. Pose estimation method proposed by Eizentals et al [15]*

A yield real time monitoring system was developed by Chang et al. (2012) that is able to map the yield of wild blueberries [16]. Blueberry precise geographic locations are found. Figure 2-6 shows the device. Using the percentage of blue pixels, they conclude there is a possibility of finding the blueberry spots. Their model heavily relies on colour data and is

specifically designed for generating blueberry yield maps, emphasizing a narrow focus within the broader farm context.

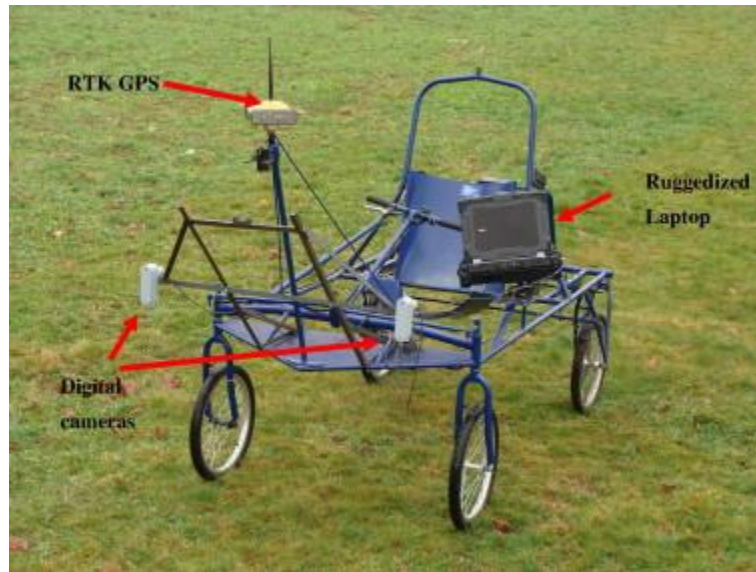


*Figure 2-6. Device configuration for automated yield monitoring system for detection of location of target plants [16]*

Davidson et al. (2016) proposed a new gripper for harvesting apples as shown in Figure 2-7 [17]. They used image processing technique to detect the apples. The accuracy of their system is 95% and the harvesting time is about 8 seconds for each apple. However, some modifications, such as expanding the workspace and mounting the device on a vehicle, are necessary to investigate the device in real orchards.

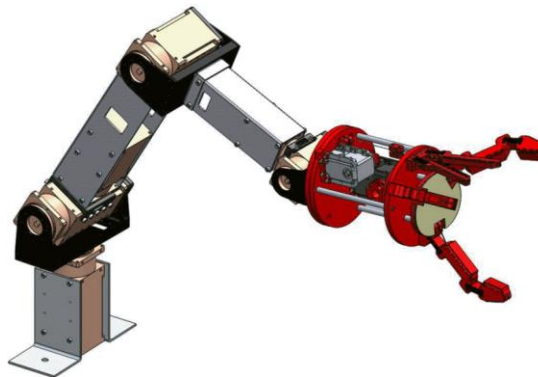


*Figure 2-7. Gripper designed for harvesting apples using a robotic arm [17]*

Based on the above review, a literature review matrix is presented in Table 2-1 to highlight the key points of their work and to position the contribution of this research.

Table 2-1. Literature review matrix

Reference	Crop: cucumber (C), Others (O)	Expandable to Multiple crops	Image preprocessing	Recognition Colour (C), Shape (S), Depth (D), Width (W), Height (H)	Detection and harvesting simultaneously	Geometry analysis	Communication Between image processing and robotic arm	Multiple models
Jing [4]	O	×	✓	C, S	×	×	×	✓
Zheng [5]	C, O	✓	✓	C, S, D	×	×	×	×
Gené-Mola [6]	O	×	✓	C, D	×	×	×	✓
Kheiralipour [7]	C	×	✓	S, C	×	✓	×	×
Rabby [8]	O	✓	✓	S, C	×	×	×	×
Liu [9]	O	×	✓	C, S	×	×	×	×
Tu [10]	O	×	✓	C, D	×	×	×	✓
Iskandar [11]	O	×	✓	C	×	×	×	×
McGuinness [12]	O	×	×	×	×	×	×	×
Yotisha [13]	O	×	✓	C	✓	×	✓	×
Shaprov [14]	O	✓	×	×	×	×	×	×
Eizentals [15]	O	×	✓	C, S, D, W, H	×	✓	×	×
Chang [16]	O	×	✓	C	×	×	×	×
Davidson [17]	O	×	✓	C	✓	×	✓	×
This study	C	✓	✓	C, S, D, W, H	✓	✓	✓	✓

### ***2.3. Research gap***

It can be seen that prior studies have focused on certain aspects outlined in the matrix. However, this study addresses complete automated cucumber harvesting, incorporating cucumber detection, a robotic arm for harvesting, geometry analysis, and communication between image processing and a robotic arm. Thus, this research establishes a foundation for all aspects of the process and offers alternative ways to compare results.

Utilizing a 3D camera, a novel preliminary study is conducted to directly manage RGB-XYZ data to find the shape of the cucumber; eliminating the need for datasets and training. Force analysis is conducted to determine the peak force that cucumbers can withstand before bruising. The study explores the impact of various parameters such as cucumber diameter and curvature.

The following chapter furnishes details regarding the methodology employed in this study to achieve the research objective.

### 3. METHODOLOGY AND TEST SETUP

This chapter begins with the introduction of the proposed model, accompanied by flow diagrams such as data and event flow diagrams. Subsequently, the essential experimental and software tools are outlined. Following this, metrics employed for image processing evaluation are presented. The artificial greenhouse is then discussed. The configuration and calibration of the 3D camera, followed by an exploration of the camera's movements are presented. The chapter further elaborates on the image processing methods, with a subsequent focus on force and geometry analyses as the final components of the research.

#### 3.1. Proposed model

The proposed model is illustrated in Figure 3-1, showcasing four primary components: 1. Image processing unit, 2. Robotic arm, 3. Cutter, and 4. Container to hold cut cucumbers.

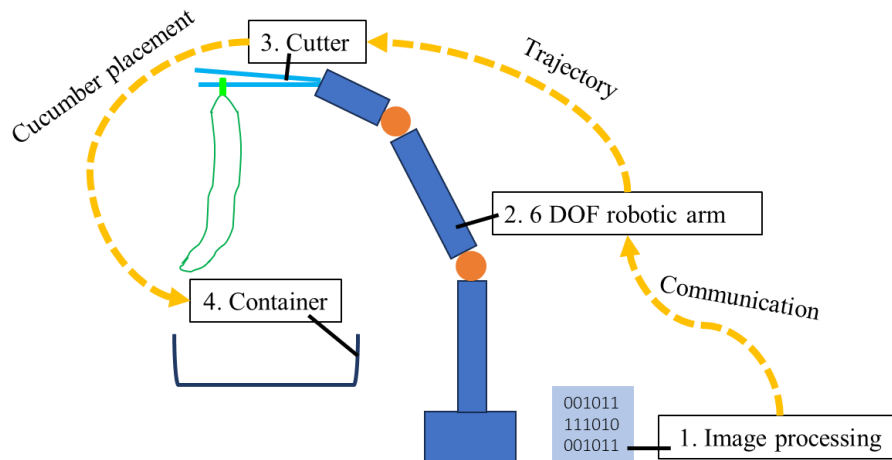


Figure 3-1. Overview of the proposed model of the automated cucumber harvester

#### 3.2. Flow diagrams of the proposed model

The flow diagram delineates the sequential steps of the automated system, from the image input to the cucumber placement. Flow diagrams are categorized into three primary types: process flow diagram, event flow diagram, and data flow diagram.

##### 3.2.1. Process and event flow diagrams

The process and event flow diagram are illustrated in Figure 3-2. Image processing unit identifies and target cucumbers. A cutting robotic arm receives the position of cucumber

through a communication system, that links the output of the image processing to the robot. Ultimately a successful cut with the cutter and the placement in a container are expected.

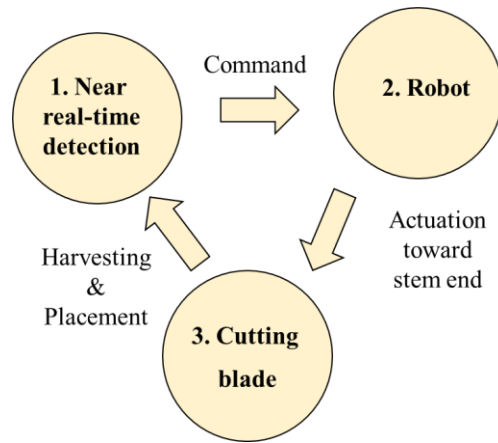


Figure 3-2. The process and event flow diagram of the proposed automated harvester

### 3.2.2. Data flow diagram

The data flow of the proposed model is also shown in Figure 3-3.a. The information related to cucumber is processed using image processing algorithm. The decision-making involves selecting the target cucumber based on the processed data. The system then transmits the position of the target stem end and trajectory information to the robotic arm for cutting. All acquired and processed data are stored in a database for further analysis and future reference, allowing continuous improvement of the system based on historical data. A flowchart of the system’s input/output and decision making is presented in Figure 3-3.b.

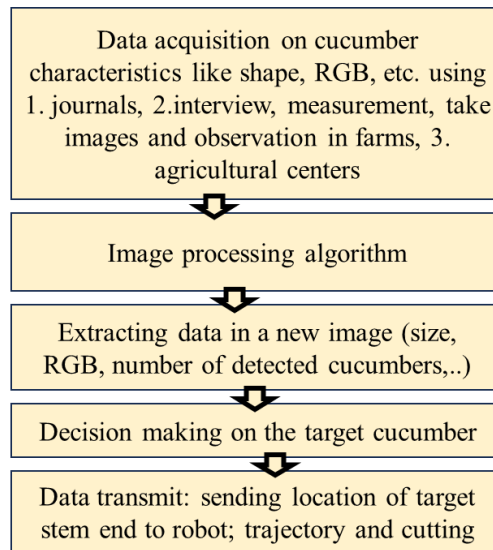


Figure 3-3. Data flow of the proposed model

### ***3.3.Experimental tools and equipment***

An overview of the experimental equipment is presented in this section.

First, the compact and lightweight robotic arm (model UR3e) which is manufactured by Universal Robots is used. The UR3e finds application in industrial settings where precision and safety are paramount, and human-robot collaboration is essential. Featuring a user-friendly programming interface, the UR3e can seamlessly integrate into various work environments, enhancing efficiency and productivity. Detailed overview on UR3e can be found in reference [18] and APPENDIX A.

An experimental tool in use is an artificial greenhouse featuring 3D printed peppers, cucumbers, and apples, with some artificial leaves and vines.

In this study, cutting blades are placed in 3D printed brackets, which are embedded in TCP of the UR3e robot. There should be an appropriate level of tightness between the TCP and the blades to prevent any slipping.

Intel's RealSense D435if camera employs LiDAR and stereo depth technologies [19]. Operating on USB 5V power, the D435if captures colour and XYZ data simultaneously, producing a point cloud for scene reconstruction. Widely utilized in machine-vision-based devices due to its compact design, this 3D camera proves particularly useful when the focus is on measuring the distance between the object and the camera.

Pressure sensors are employed to measure the maximum force cucumbers can withstand, determining their tolerance before permanent damage. This study employs two types of sensors: finger type, utilized for cutting and gripping forces when applied parallel to the cucumber cross-section, and plate type, employed for examining the length and curvature effects of cucumbers with applied force normal to the cross-section.

To mount the camera on the UR3e arm, a bracket is 3D printed. The optimal position for the camera on the robot is determined, and subsequently, the dimensions and shape of the bracket are obtained. The bracket is then 3D printed using 3D printer (model Creality-Halton-Mega Pro).

### ***3.4.Software tools***

The following section provides information about software tools.



The YOLO architecture has undergone several iterations, each bringing about improvements in accuracy, speed, and versatility. YOLOv8 introduced by Ultralytics has new features and improvements for enhanced performance, flexibility, and efficiency that support a full range of vision AI tasks [20]. These tasks include detection, segmentation, pose estimation, tracking, and classification. In this study, both pose estimation and object detection models are employed.

RealSense SDK software is used to configure D435i cameras. The software should be installed after connecting the 3D Webcam D435i to the computer.

Roboflow is an automated platform designed to streamline object detection, image classification, and segmentation. Roboflow provides a range of pre-defined tools for dataset preparation, such as resizing, labeling, cropping, annotation, and augmentation.

The Dynamic Calibrator software from Intel is specifically designed for the calibration of D435 series cameras.

MATLAB is employed for geometry analysis, with specific emphasis on utilizing the Curve Fitting Toolbox.

Two programming methods include graphical programming interfaces (arranging and sequencing predefined commands from a library) and teach pendants (manually manipulating the end-effector to instruct the robotic arm) are used.

SolidWorks software is used for design artificial peppers, apples, and cucumbers and brackets before 3D printing.

Python is a programming language commonly employed for developing applications, including those in machine learning and image processing. Python can be employed to implement or interact with YOLO-based object detection algorithms.

RStudio serves as the tool for analyzing literature and establishing the study's context. Functioning as a platform for the R programming language, RStudio is specifically designed for statistical analysis within datasets.

WIDACS software connects the pressure sensors to a PC. The software records force variations, pinpointing the moment when the cucumber is damaged.

CVAT is utilized for labeling images intended for image processing purposes. Prior to training, it was necessary to label cucumbers..

### ***3.5.Metrics in image processing evaluation***

Precision, recall, and F1 score are fundamental metrics used in evaluating object detection models, providing insights into their performance regarding true positive (TP), false positive (FP), and false negative (FN) predictions. Precision, denoted as the ratio of TP to the sum of TP and FP, measures the model's accuracy in correctly identifying positive instances. Recall, calculated as the ratio of TP to the sum of TP and FN, assesses the model ability to capture all relevant positive instances. F1 score, representing the harmonic mean of precision and recall, offers a balanced assessment of a model's overall performance by considering both false positives and false negatives.

### ***3.6.Artificial greenhouse***

An artificial greenhouse for testing the harvester and for identifying potential drawbacks is fabricated. In summary, the test environment aims to:

- Implement the image processing unit and cutting robotic arm.
- Validate the setup under various light conditions.
- Prepare the harvester for real-world scenarios, such as hidden cucumbers.
- Ensure there is a setup for future development, including the detection of peppers.

Initially, artificial cucumbers, peppers and apples are manufactured using additive manufacturing. CAD files before 3D printing of them are depicted in Figure 3-4 [21].

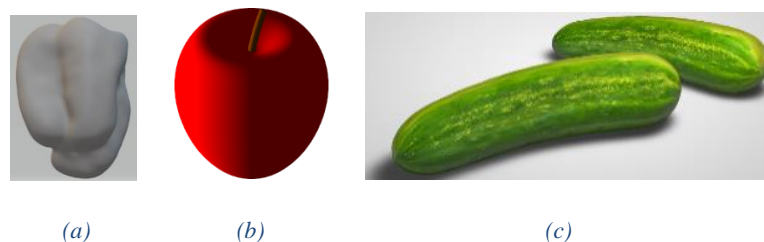


*Figure 3-4. Sample CAD files for the artificial: a. peppers, b. apples, and c. cucumbers before 3D printing*

The 3D printed peppers, apples, and cucumbers are showcased in Figure 3-5. Attaching the stem ends to them requires a post-processing step involving drilling, as depicted in Figure 3-5.

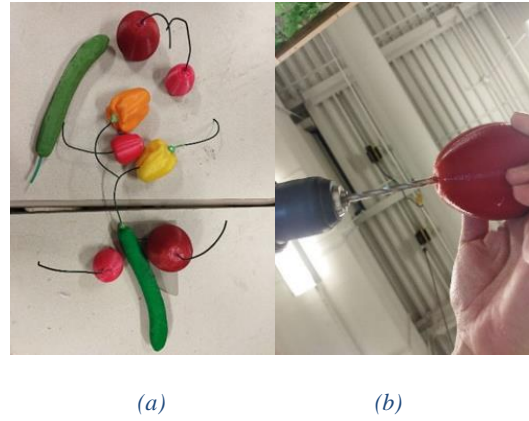


*Figure 3-5. a. 3D printed peppers, cucumbers, and apples, and b. The post-processing*

After manufacturing peppers, cucumbers, and apples, they are integrated into a frame along with leaves, as shown in Figure 3-6. The drawback of this artificial greenhouse is that produce doesn't grow in this manner (multiple types on one vine). However, since only cucumbers are the focus of this study, this artificial greenhouse contributes to the feasibility of the model. Artificial Peppers and apples are for future studies.



*Figure 3-6. In-house artificial setup*

### ***3.7. Camera setup and calibration***

Detailed information regarding camera setup and specifications is provided in APPENDIX B. Intel has developed the Dynamic Calibrator software for calibrating D435 series cameras. The process involves connecting the camera to a laptop, launching the RealSense software, and transitioning to 2D mode for simultaneous access to RGB and 3D modes.

The calibration utilizes the Intel RealSense Calibration Print Target. Running the Intel RealSense Dynamic Calibrator software involves positioning the printed target in various orientations, directions, and distances for XYZ mode calibration as shown in Figure 3-7. The process for calibrating RGB mode follows a similar approach, with the RGB calibration interface. A comprehensive camera calibration process is outlined in APPENDIX C.

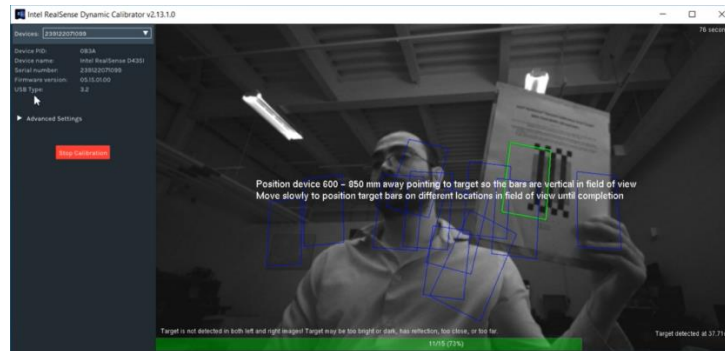


*Figure 3-7. The dynamic calibration print target should be placed in 16 different positions for camera calibration*

### ***3.8. Camera and cutter movement control using UR3e***

In this study, the motion of camera and cutter is controlled by graphical programming interfaces and teach pendants of UR3e. An experimental test is conducted wherein the D435if camera is mobilized using the UR3e robot. The RealSense software records the scanning process. The robot is programmed to scan at various angles and sides, acknowledging that a cucumber may be visible from one angle but concealed by leaves from another side. The results are presented in Figure 3-8.



*Figure 3-8. Camera movement at different angles and directions*

If the camera moves too quickly, the D435i's limitations may lead to the cucumber being invisible. On the other hand, moving too slowly can result in wasted time. The UR3e offers the flexibility to set different speeds for the TCP where the camera is positioned. A speed between 50 and 70 mm/s is recommended based on this test.

### ***3.9.Object detection using popular pretrained models***

For accurate object detection, pretrained models have become a common practice. Pretrained models are neural networks that have undergone training on extensive datasets for general tasks, such as image classification. The pretrained model excels in extracting high-level features from images, enabling the detection of complex patterns and objects. They significantly reduce training time compared to training a model from scratch.

Three of the popular pretrained models are explored with their characteristics and their advantages and they are summarized in Table 3-1.

*Table 3-1. Comparison between three of popular pretrained models*

Pretrained model	Characteristics	Advantages
SSD	Multiscale feature extraction, narrow down target in each stage	<ol style="list-style-type: none"> <li>1. Balance between speed and accuracy</li> <li>2. Handling different object sizes</li> </ol>
Faster R-CNN	Two-stage approach: 1. RPN, 2. Final object detection	<ol style="list-style-type: none"> <li>1. High accuracy</li> <li>2. Better handling of complex object detection</li> </ol>
YOLO	Single-pass approach	<ol style="list-style-type: none"> <li>1. Real-time detection</li> <li>2. Fast response</li> <li>3. Easy to implement</li> <li>4. Diverse range of objects</li> </ol>

Based on Table 3-1, YOLO has the capability to rapidly detect cucumbers in near-real-time scenarios, and its ease of implementation makes it the chosen approach for this study. The process is elaborated in the rest of the text.

### **3.10. *Cucumber bounding box detection using two models in YOLOv8***

The bounding box method is the most prevalent approach to fruit detection, as per the literature. It entails creating a rectangle around the detected cucumbers. Different models in YOLOv8 are applied to detect cucumber bounding box. These configurations differ in the size and complexity of the model, allowing users to choose a version that aligns with specific trade-offs between computational efficiency and detection accuracy. The object detection task begins with camera calibration and data preparation. To fulfill object detection task, two distinct custom datasets are used. Artificial Cucumber Greenhouse dataset includes synthetic representations of cucumber greenhouses. The second dataset, known as the Real Cucumber Greenhouse dataset includes images captured within real cucumber greenhouses. YOLOL and YOLON are utilized for bounding box detection. The difference between them lies in their performance characteristics. YOLOL is known for its accuracy but demands more processing time and a more robust computer. On the other hand, YOLON is a lighter and faster model, but typically sacrifices some accuracy compared to YOLOL.

For annotation and labeling of objects within these datasets, CVAT is utilized [22]. The use of CVAT facilitated a systematic and accurate labeling process. An instance of the labeled cucumbers in CVAT are shown in Figure 3-9. After annotating images, they are fed into YOLO models, which undergo training. Subsequently, these models are tested with new images, and the identified cucumbers and metrics are showcased in the results section. The resulting output consists of images containing bounding boxes, accompanied by corresponding text files, called Json file. These text file has the position information of the detected cucumber.



*Figure 3-9. An example of labeled cucumbers using CVAT*

### **3.11. *Cucumber keypoints detection using two models in YOLOv8***

Pose estimation and highlighting keypoints are critical tasks in computer vision, involving the determination of the spatial position and orientation of objects or humans in an image or video [23]. The whole process is like bounding box detection other than the labelling approach. Labeling involves outlining rectangles around the cucumbers in a dataset before commencing the model training process. For cucumber pose estimation, three keypoints of each cucumber: top, bottom, and middle points are labelled. Each cucumber in the dataset is labeled with these three keypoints. Here, only YOLOX and YOLOL are applied. The only distinction between them is that YOLOL is faster compared to YOLOX, but it is less accurate.

### **3.12. *Cucumber bounding box detection using one model in RoboFlow***

Roboflow simplifies the preparation of image datasets for research purposes, offering key features. Users can easily import image datasets, whether they are stored locally or in the cloud. Cucumber detection requires labeling of regions containing cucumbers. Roboflow provides annotation and labeling tools for this purpose.

### **3.13. *Cucumber shape detection using raw RGB-XYZ data***

In this part, the output from the 3D camera (RGB-XYZ data) is partly managed using Python. First, conducting a colour analysis on the target cucumber and plant components is done. After filtering, the target RGB values for cucumbers are kept and other RGBs related to vines and leaves are removed as shown in Figure 3-10. Some pixels of cucumber are mistakenly filtered out (false negatives), while some pixels of leaves and vines are

inaccurately identified as cucumber pixels (false positives), as shown in Figure 3-10. By eliminating false positives and retaining false negatives, the final remaining RGBs form a cucumber shape.

Then, XYZ data comes into the picture. Using XY data, the sizes of cucumbers and the position of the stem end are identified. With Z data, the distance between the robot and the cucumber is determined. This process can be handled using Python. More details are provided in APPENDIX D.

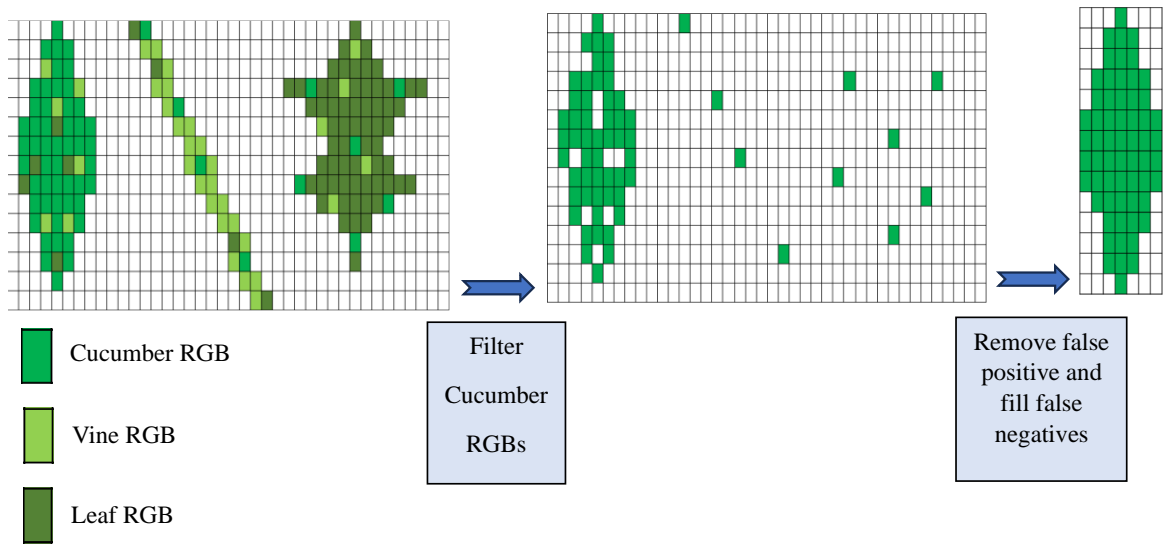


Figure 3-10. Left: visualization of target RGB values for cucumber, vine, and leaf (each square assumed to be a pixel). Middle: false positives and false negatives pixels. Right: after removing false positives and retaining false negatives, a complete cucumber shape is maintained, while all leaves and vines effectively filtered out

### 3.14. Communication between image processing and robotic arm

The third component of the automated cucumber harvester is the interface between image processing and the robotic cutting arm. After detecting the position of cucumber, the robotic cutting arm initiates its movement for harvesting. In this study, a JSON file containing the X and Y positions of the cucumber is generated through YOLO. Subsequently, the obtained position is manually input to the robot. Upon receiving the position data, the cutting robotic arm initiates movement towards the stem end, executing the cutting process. The outcomes are detailed in the results section. More details on different possible interface in UR3e are presented in APPENDIX E.



### 3.15. *Force analysis using pressure sensors*

Force analysis is essential to avoid any damage on the cucumber when placing it in a container and when cutting it from the stem end. The aim is to investigate the forces that cucumbers can withstand. This information is useful for designing the container and determining the appropriate distance between them and the cucumbers to ensure that the cucumbers remain undamaged when falling into the container. Undamaged cucumbers are those without any trace of distortion on their surfaces resulting from harvesting. More details on the container are provided in APPENDIX F.

Pressure sensors are employed to measure the maximum force that different types of cucumbers can endure. The experimental setup used to measure this force and an example of a damaged cucumber after applying force are shown in Figure 3-11. The WIDACS software is installed, and forces on cucumbers are manually put to the pressure sensors. The results are presented in the results section.



*Figure 3-11. a. Experimental setup to find the peak forces that each cucumber can tolerate and a damage cucumber after applying force, b. Damaged cucumber after applying force on its surface*

### 3.16. *Geometry analysis with MATLAB*

Understanding the shape of target cucumbers is crucial. The identification of cucumber sizes is dependent on determining the curve that fits the cucumber's boundaries and acquiring specific data points. The method involves utilizing 3D shape data obtained from a 3D camera and the use of MATLAB. In this approach, curves are fitted to various images of cucumbers utilizing the curve fitting toolbox in MATLAB. The curve can take different orders. The results of this analysis are shown in chapter results.

The following chapter presents the results and outcomes obtained through the application of the methodology and test setup discussed in the preceding section.

## 4. RESULTS AND DISCUSSION

This chapter delves into the outcomes of image processing employing four models in YOLOv8, encompassing corresponding qualitative and quantitative outputs. The findings of near-real-time detection in YOLOv8 are also shown. The chapter also incorporates findings related to programming the cutting arm. Geometry and force analyses results, contributing to a comprehensive understanding of cucumber characteristics, are also showcased. Finally, a comparison between manual and automated processes is established through cost and OEE analyses.

### ***4.1. Cucumber bounding box and keypoints detections using YOLOv8***

The examination of cucumber bounding box and keypoints detections is conducted, and qualitative and quantitative results are showcased.

#### ***4.1.1. Bounding box***

As discussed in the literature review and methodology chapters, the use of bounding boxes stands out as one of the most prevalent methods for cucumber detection. The procedural steps are expounded upon in the methodology chapter, and in this section, the outcomes are showcased through the application of two distinct models. The resultant metric for each model is also presented. Figure 4-1 displays two images in which cucumbers are detected in YOLOL (YOLO Large) model, accompanied by their respective detection confidence for each cucumber. As evident from Figure 4-1, there is no false positive in detection. However, few false negatives are observed, primarily because very small portions of cucumbers are visible in some cases. The percentage of correctness for each detected cucumber bounding box is shown in the figure. A higher percentage indicates a higher priority for harvesting that cucumber. For future decision-making regarding which cucumber to harvest in each camera capture, this information is essential. In another capture from a different angle and camera position, a different cucumber may receive a higher percentage. Therefore, that would be the priority in that capture.

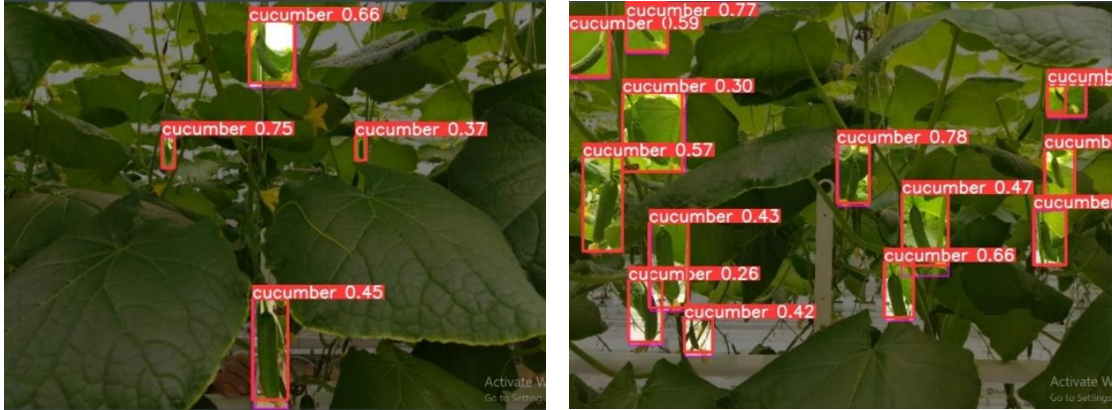


Figure 4-1. YOLOL: two images with their detected cucumbers and their confidences

F1, which is defined in methodology section, and confidence relationship is showed in Figure 4-2. Although it shows a F1 of 0.55, which shows a great balance between precision and recall, the confidence of 0.204 is pretty low.

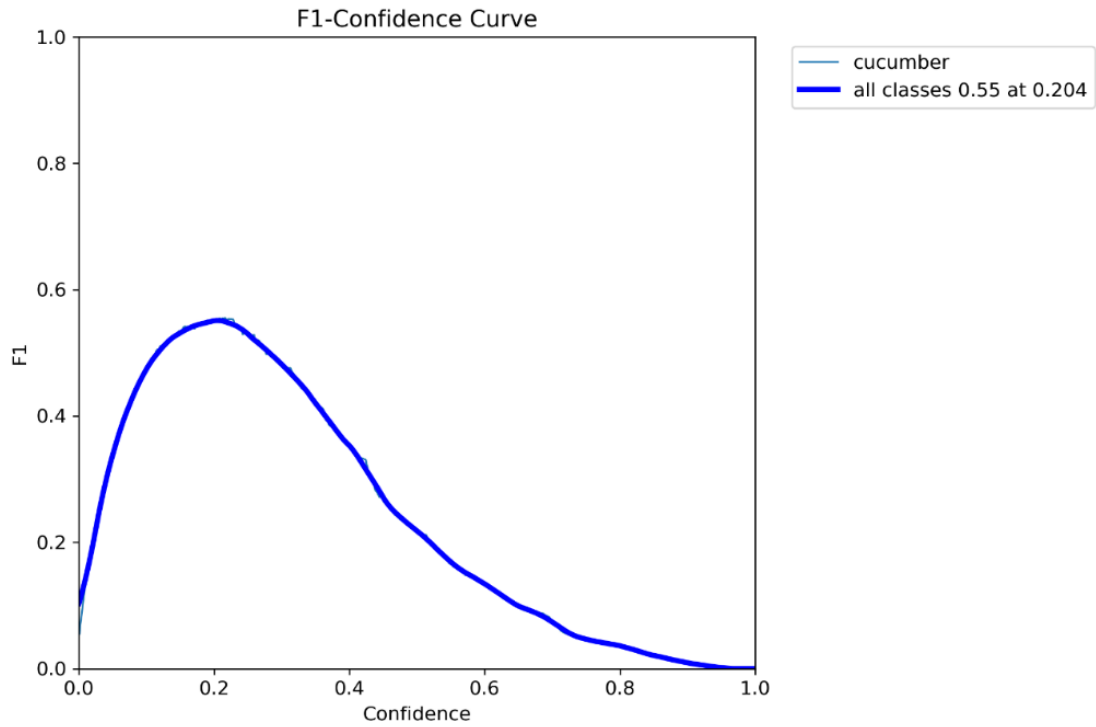


Figure 4-2. F1-confidence curve in YOLOL

Figure 4-3 illustrates two images with detected cucumbers in YOLON, along with their corresponding detection confidence for each cucumber. As is visible in Figure 4-2, like

YOLO model, there are no false positives. Nonetheless, few instances of false negatives are noted.

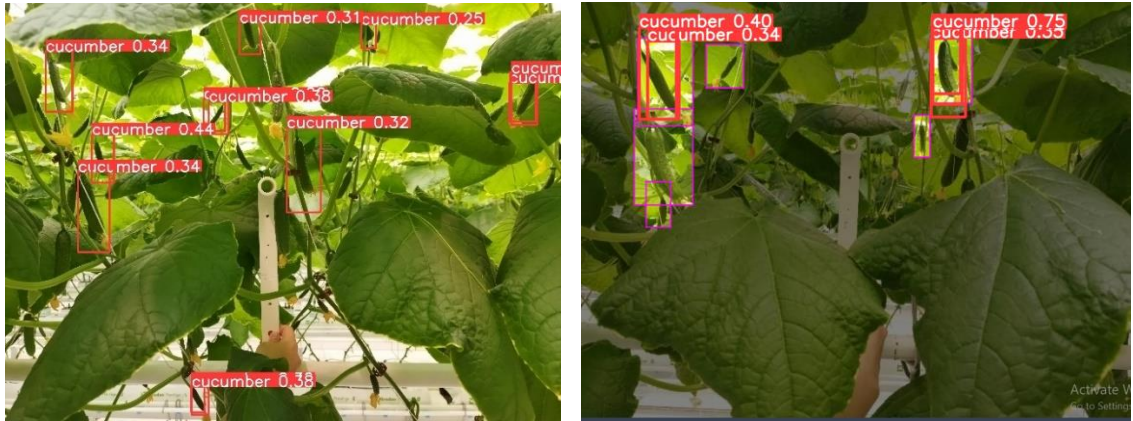


Figure 4-3. YOLON: two images with related detection confidences

Figure 4-4 displays the F1-confidene curve obtained in YOLON. Based on this graph, the best F1 score is 0.38 at a confidence of 0.121. The F1 score shows a fair trade-off between precision and recall.

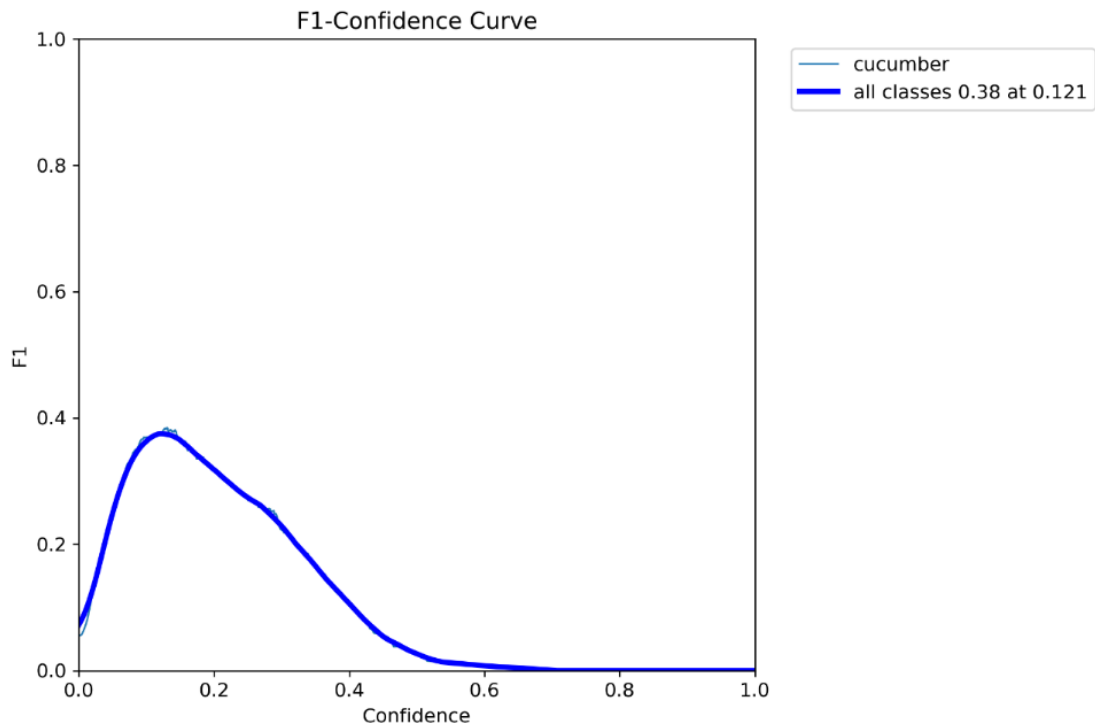


Figure 4-4. F1 and confidence relationship in YOLON

The summary of the metrics for cucumber bounding box detection is presented in Table 4-1.

Table 4-1. Summary of metrics for cucumber bounding box detection

Model	F1	Confidence
YOLOL	0.55	0.204
YOLON	0.38	0.121

#### 4.1.2. Near-real-time cucumber detection using YOLON

Cucumbers have been identified in a brief video captured at JEM Farms. Selected frames from the video are presented in Figure 4-5 (a) through (e). The speed of the video is a challenge here because it was mainly recorded for data collection purposes rather than for detection, which may be one reason of presenting many false negatives. Nevertheless, there are no examples of false positives. Moreover, almost always, at least, one cucumber is detected for harvesting in near-real-time detection.



(a)



(b)



(c)



(d)



(e)

Figure 4-5 (a) through (e). Near-real-time cucumber detection in a video from real greenhouse using YOLOL

#### ***4.1.3. Cucumber keypoints detection with YOLOv8***

In this section, the results of keypoints detection are presented using YOLOL and YOLOX models. Qualitative results and F1-confidence curves for each model are depicted in Figures 4-6 to 4-8. As indicated in Figure 4-6, the confidence level for the majority of detected cucumbers in YOLOL is notably high. With an F1 score of 0.82 and a confidence of 0.502, YOLOL exhibits promising performance, as shown in Figure 4-7. Conversely, a lower F1 score of 0.42 with a confidence of 0.053 suggests that YOLOX is not performing as effectively as YOLOL, as shown in Figure 4-8.





(a)

(b)

Figure 4-6. Detecting the cucumber pose and identifying keypoints to determine the position of the stem end in YOLOL (a), and YOLOX (b)

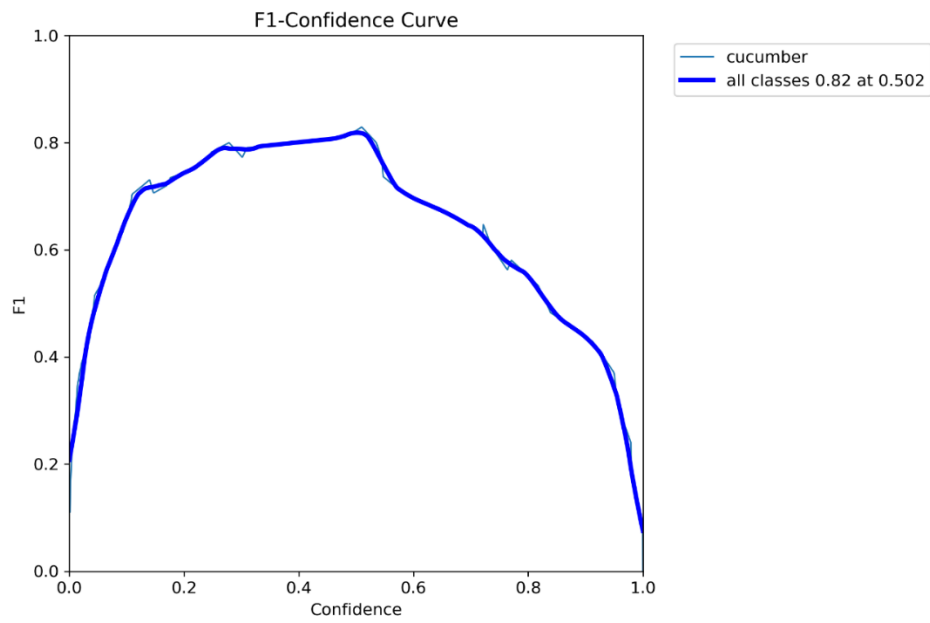


Figure 4-7. F1 and confidence graph in pose-YOLOL

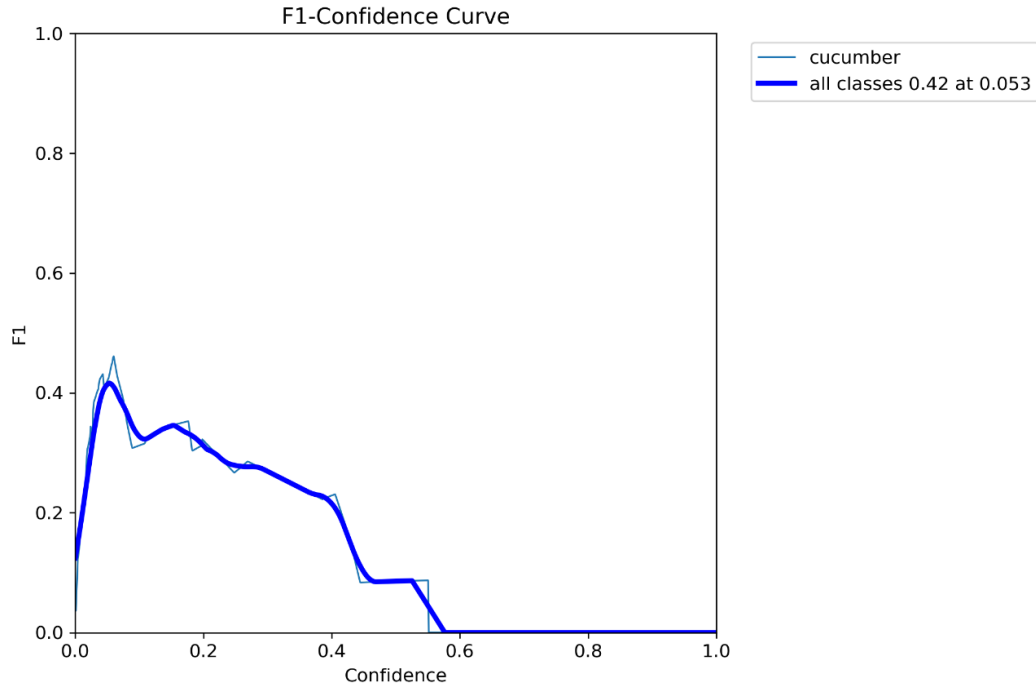


Figure 4-8. F1 and confidence relationship in pose-YOLOX

The summary of the metrics for cucumber keypoints detection is presented in Table 4-2.

Table 4-2. Summary of metrics for cucumber keypoints detection

Model	F1	Confidence
YOLOL	0.82	0.502
YOLOX	0.42	0.053

#### 4.2. Robotic arm movement

As stated in the methodology section, upon detecting a cucumber, YOLO generates a JSON file containing XY data. Subsequently, the robotic arm is programmed to move towards the identified stem end for harvesting. The outcomes of this test are similar to what is illustrated in Figure 4-9.



(a)



(b)



(c)



(d)



(e)

*Figure 4-9. a through e. Robot trajectory to harvest detected cucumbers based on received position data*

Utilizing the outcomes of image processing and the trajectory of the robotic arm, the ultimate flowchart outlining the process is depicted in Figure 4-10.

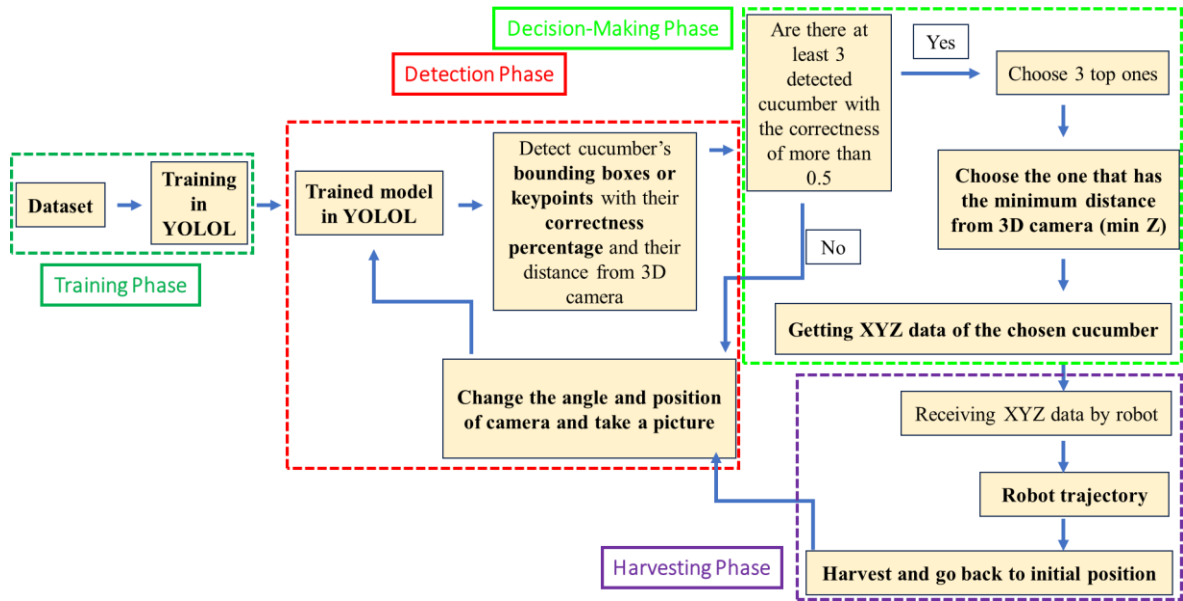


Figure 4-10. Final flowchart of the system including input/output, decision-making and harvesting

### 4.3. Geometry MATLAB analysis results

The geometry analysis using MATLAB is outlined in this section. The detailed data related to this analysis is available in APPENDIX G.

The image of the initial cucumber sample captured by the D435i camera is depicted in Figure 4-11.

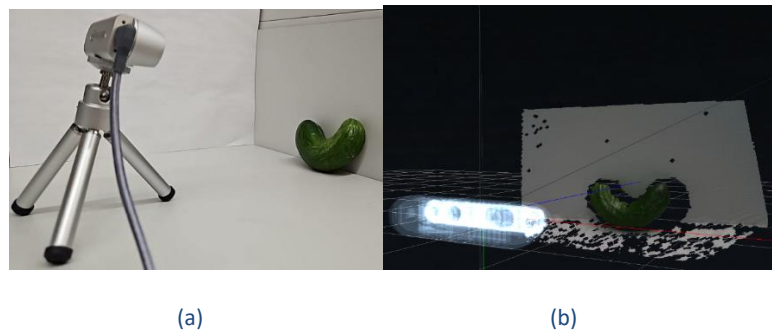
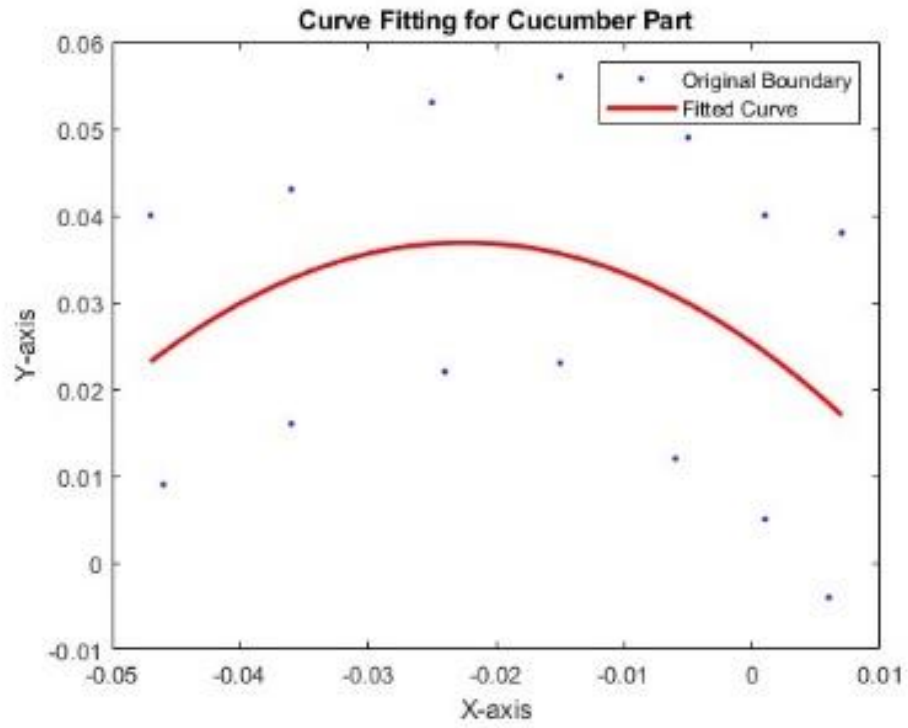
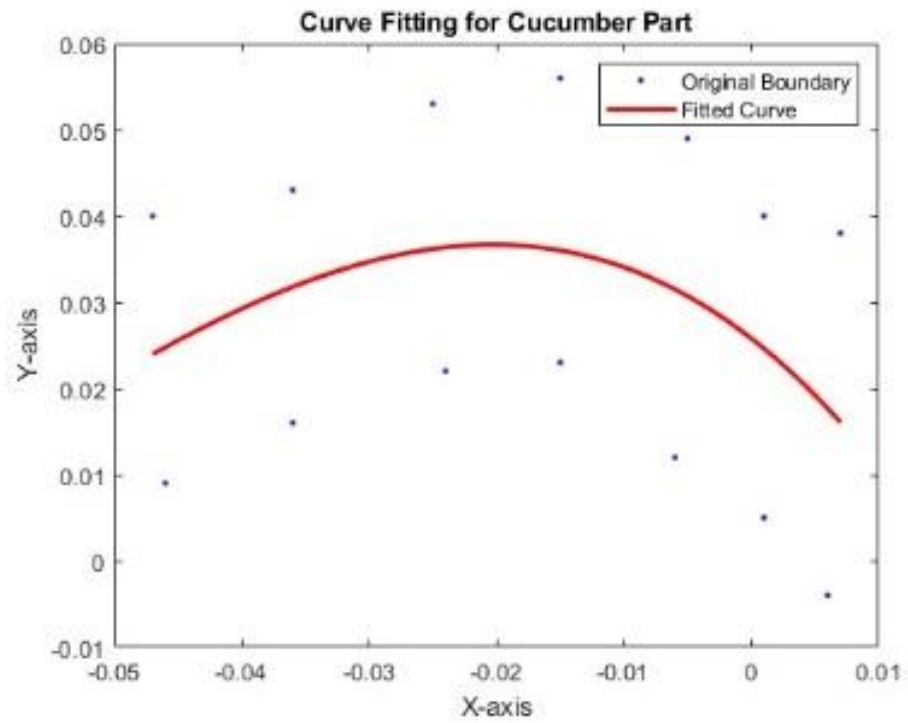


Figure 4-11. the experimental arrangement for the initial cucumber sample (a), and the resulting image displayed in the RealSense software (b)

MATLAB curve fittings of orders 2 and 3 are displayed in Figure 4-12, which show a good representation of the real cucumber geometry.



(a)



(b)

Figure 4-12 MATLAB curve fittings of orders 2 (a) and 3 (b) for first cucumber sample

The image captured by the D435if camera of the second cucumber sample is depicted in Figure 4-13. Curve fittings of degrees 2 and 3 for the second cucumber sample are shown in Figure 4-14. The curves do not exhibit a satisfactory fit for the cucumber. Perhaps, higher-order or spline curves are required. This is a future research activity if this is considered significant.

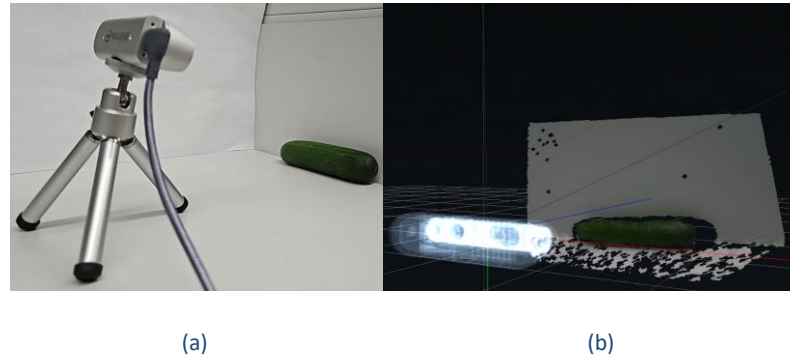
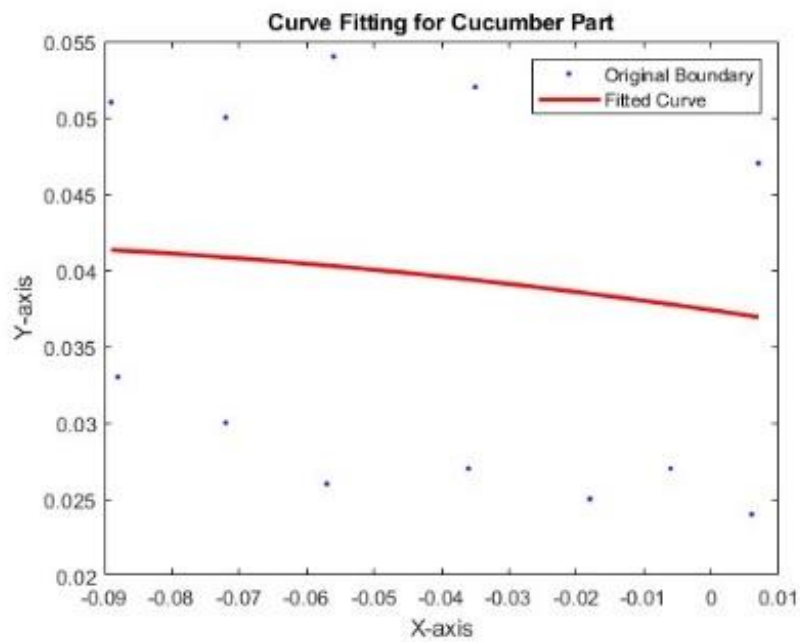
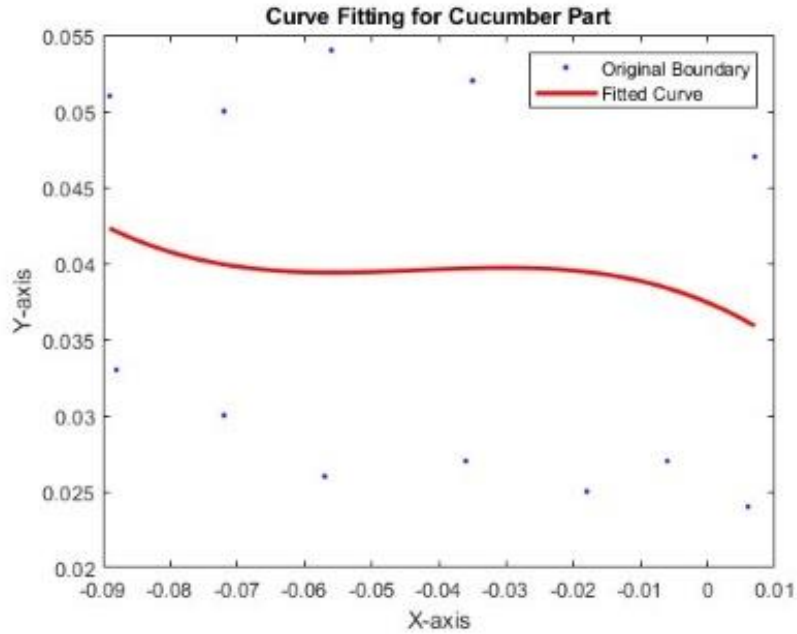


Figure 4-13 The experimental setup for the second cucumber sample (a) and the resultant image exhibited in the RealSense software (b).



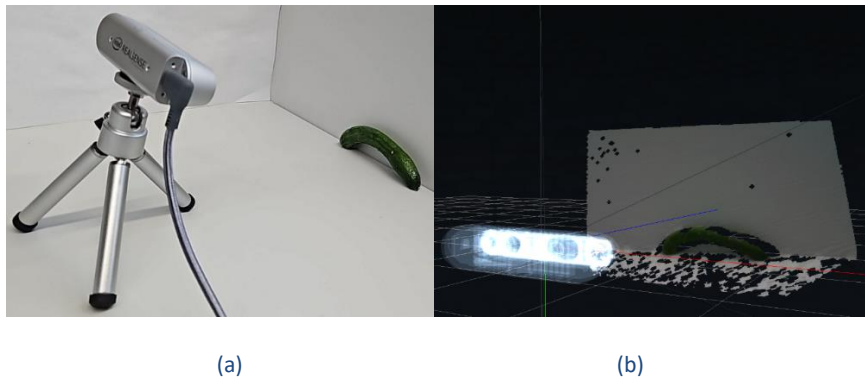
(a)



(b)

Figure 4-14 MATLAB curve fittings of degrees 2 (a) and 3 (b) for the second cucumber sample.

The image captured from the D435if camera depicting the third cucumber sample is illustrated in Figure 4-15.



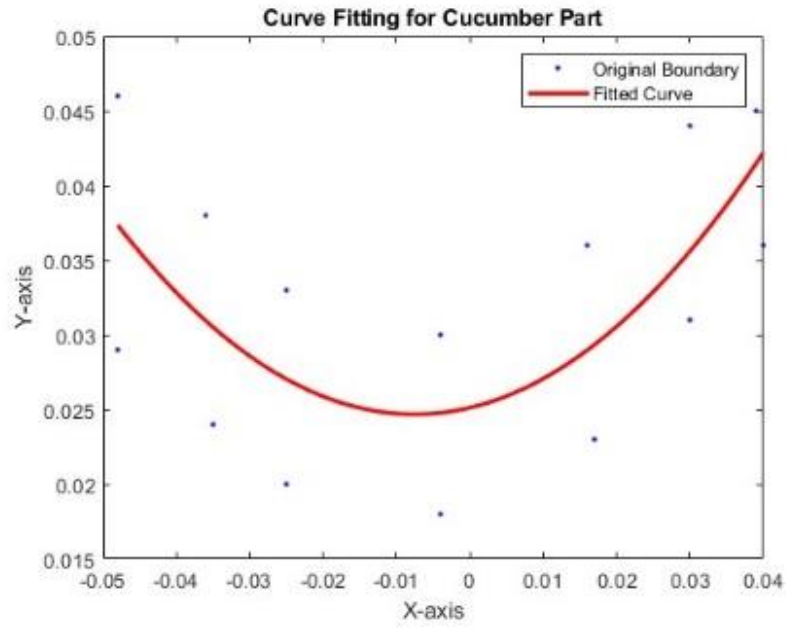
(a)

(b)

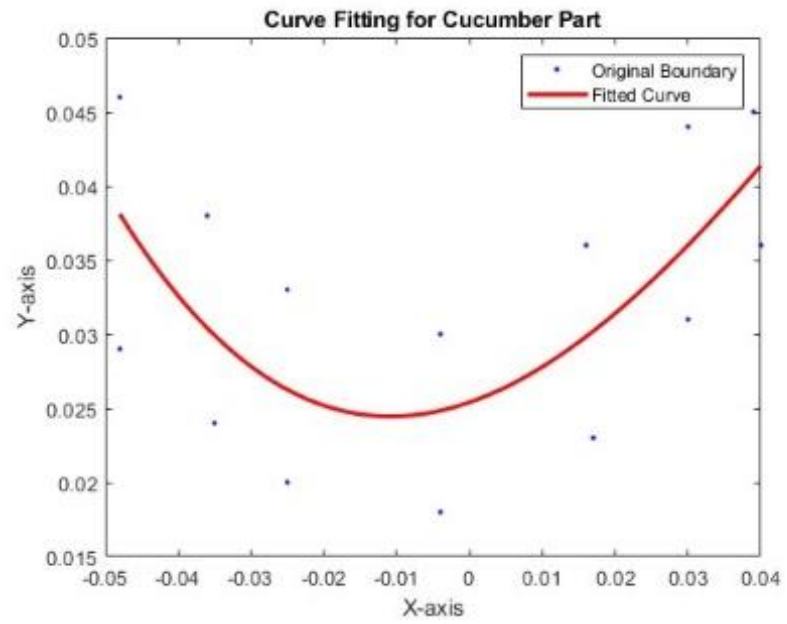
Figure 4-15 The experimental arrangement for the third cucumber sample (a) and the resulting image displayed in the RealSense software (b).

MATLAB curve fittings of orders 2 and 3 are displayed in Figure 4-16 and they show a good fit for all orders.





(a)



(b)

Figure 4-16. MATLAB curve fits of orders 2 (a) and 3 (b) for the third cucumber sample.

The image captured by the 3D camera of the fourth cucumber sample is shown in Figure 4-17. MATLAB curve fittings of orders 2 and 3 are presented in Figure 4-18. They show a good fit, no matter in which order.

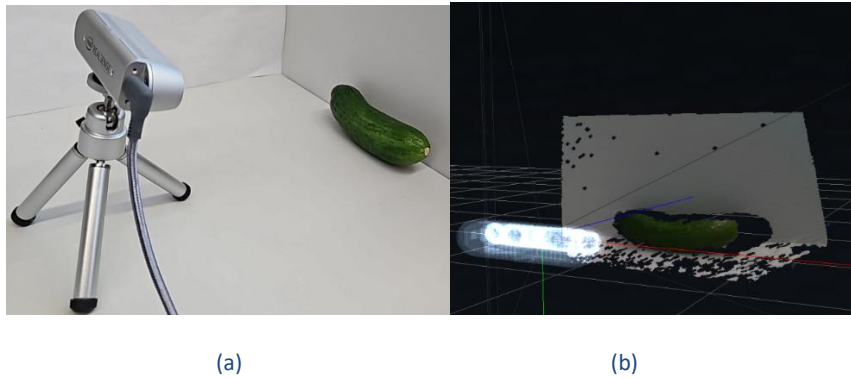
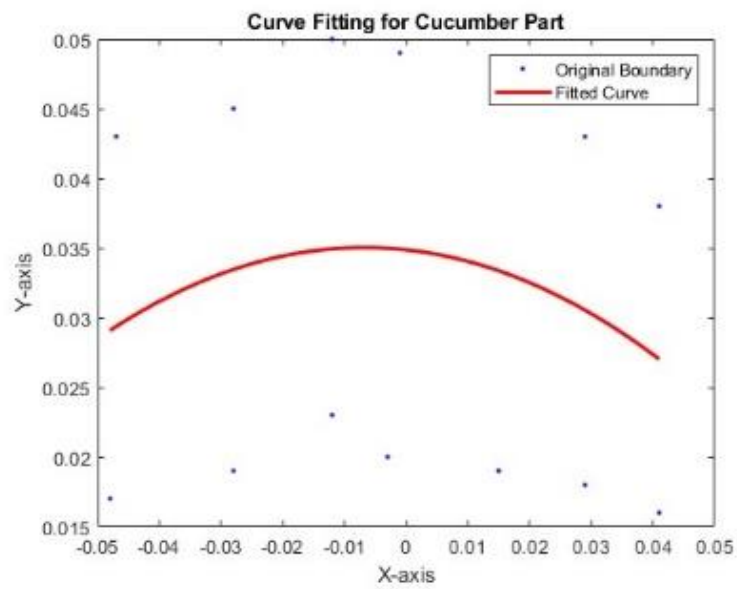
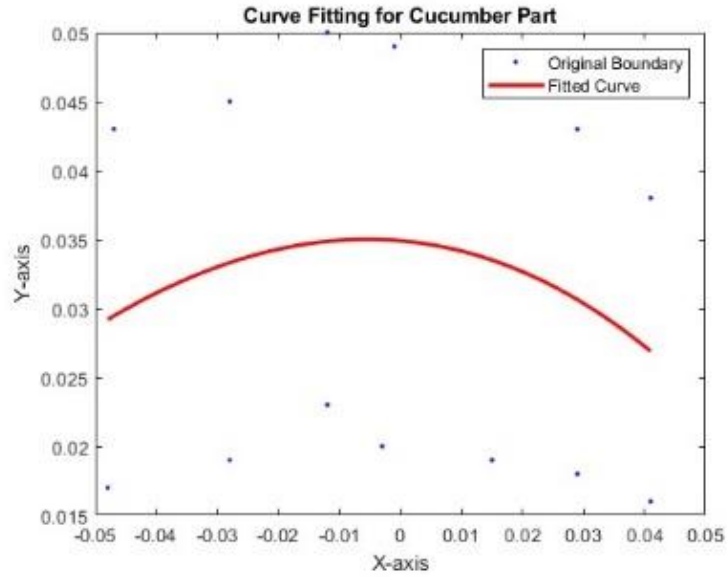


Figure 4-17 The experimental setup for the fourth cucumber sample (a), along with the resultant image showcased in the RealSense software (b).



(a)



(b)

Figure 4-18 MATLAB curve fittings with orders 2 (a) and 3 (b) for the fourth cucumber sample.

The image taken by the camera of the fifth cucumber sample is shown in Figure 4-19.

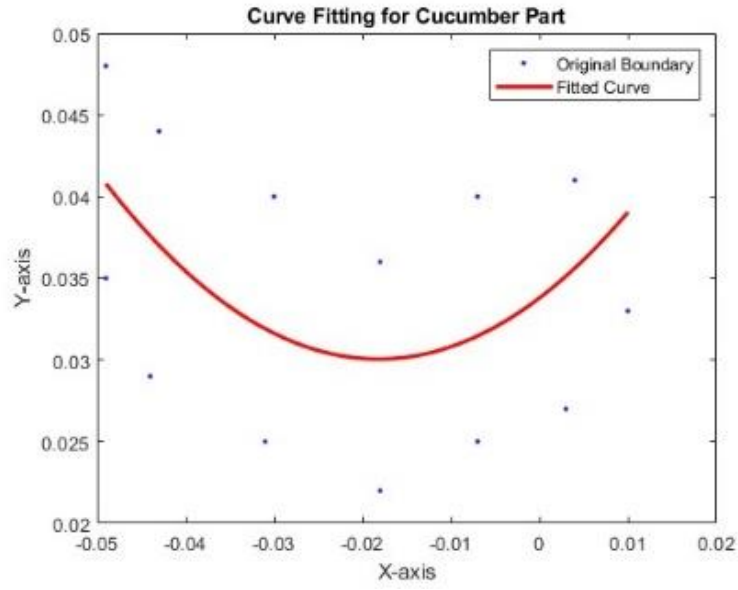


(a)

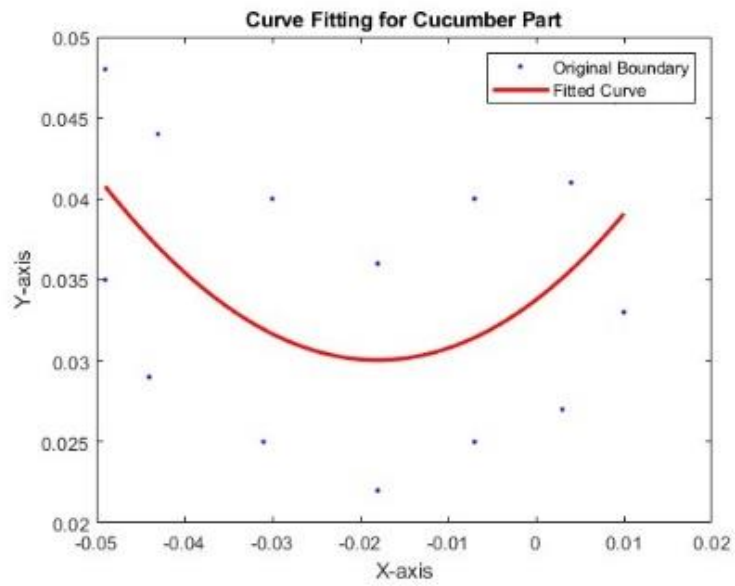
(b)

Figure 4-19 The experimental configuration for the fifth cucumber sample (a), accompanied by the resulting image displayed in the RealSense software (b).

MATLAB curve fittings of orders 2 and 3 are displayed in Figure 4-20, they show a good fit with real cucumber boundaries.



(a)



(b)

Figure 4-20. MATLAB curve fittings of degrees 2 (a) and 3 (b) for the fifth cucumber sample

#### 4.4.Managing RGB-XYZ data in Python

A total of 13,806 unique R, G, and B values are identified in images captured from the JEM farm, categorized into two types; type 1 is long English cucumbers and type 2 is small

regular cucumbers. Intervals of RGB values of cucumbers, stem ends, vines, and leaves are presented in Tables 4-3 and 4-4.

*Table 4-3. RGBs' intervals for type 1 plant's components*

	Red interval	Green interval	Blue interval
Cucumber	(61.6-81.2)	(55.7-74.7)	(44.1,69.9)
Stem end	(62.3-109.2)	(61.4-104)	(39.7-83)
Vine	(105-148.7)	(115.4-148.6)	(39.2-97.8)
Leaf	(91.4-122.8)	(112.4-151)	(43.7-95.5)

*Table 4-4. RGBs' intervals for type 2 plant's components*

	Red interval	Green interval	Blue interval
Cucumber	(42.8-88.3)	(52.2-108.9)	(7.6-36.3)
Stem end	(73-139.6)	(98.3-158.8)	(8.9-78.2)
Vine	(90-151.5)	(115.4-167.2)	(17.9-50.2)
Leaf	(70.4-123.1)	(107-148.4)	(14.9-53.9)

A Python script is developed to filter the red, green, and blue intervals of cucumbers, as outlined in Tables 4-3 and 4-4. Following the retention of only the RGB values of cucumbers, the pixels are then successfully sorted based on their Z value.

#### ***4.5. Force analysis***

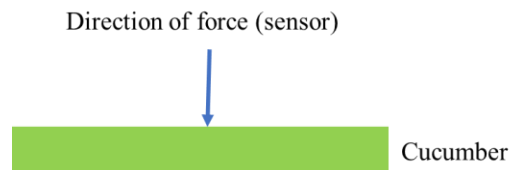
Following the experimental setup outlined in the methodology chapter, a force test is conducted on the cucumber samples as depicted in Figure 4-21.



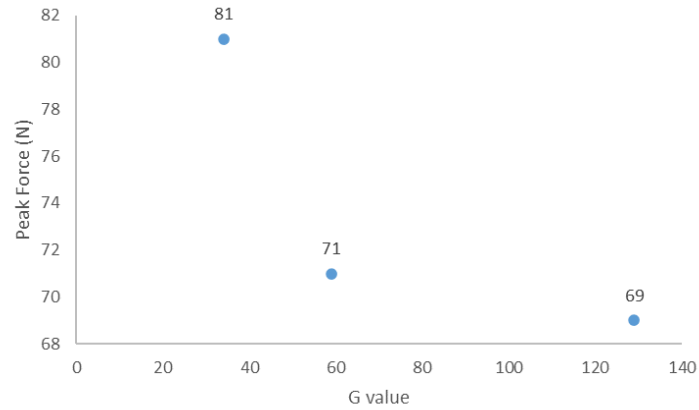
Figure 4-21. Samples for experimental test on peak tolerable force

Finger pressure sensor is used for all experiments other than when examining the effect of curvature and length on peak axial load, where the plate pressure sensor is used. After applying force, the variation of force is recorded as a parameter of time. After seeing the first trace of damage on the cucumber, the force is stopped. The impact of certain parameters is presented in the following paragraphs.

In the initial test, force tests are conducted on three cucumbers with different G values (Green colour values). All other parameters are consistent across these cucumbers. The direction of applying force and the final peak load for each sample is determined and presented in Figure 4-22. It appears that as the G value increases, the peak load before observing any signs of damage on the cucumber also increases.



(a)



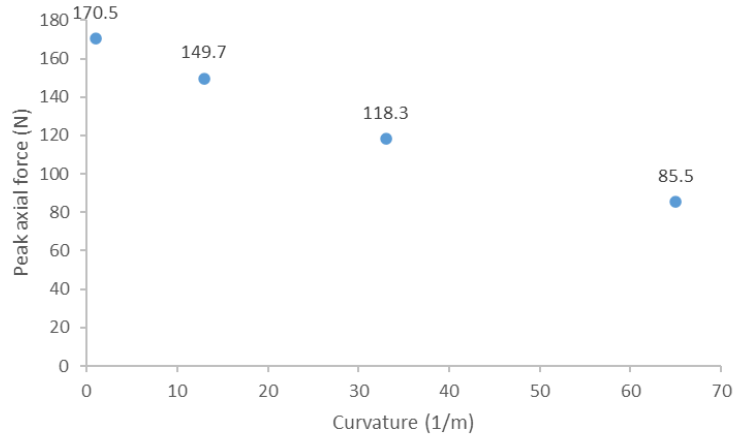
(b)

Figure 4-22. a. The direction of applying force, and b. The effect of colour on peak load

The influence of curvature on axial peak load is investigated. Four cucumbers with varying degrees of curvature undergo testing, and the peak load results are depicted in Figure 4-23. All parameters remain consistent across these cucumbers. From the graph, it is evident that straighter cucumbers can withstand more axial force. This is a predictable outcome as buckling is less likely to significantly impact straight cucumbers.



(a)



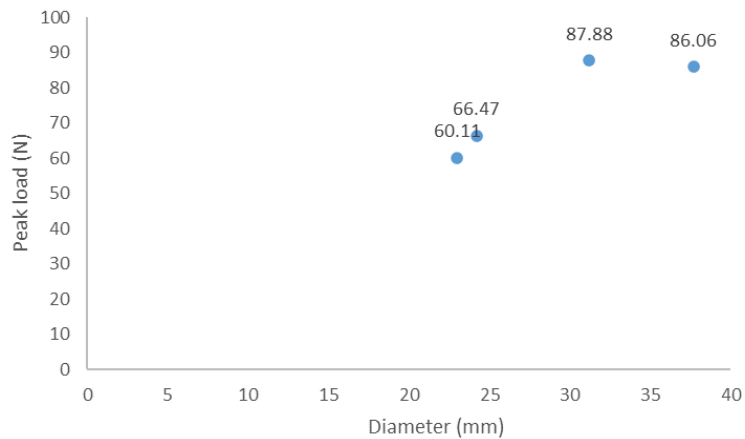
(b)

Figure 4-23. a. The direction of applying force, and b. The effect of curvature on peak axial load

Four cucumbers with varying diameters undergo testing, and the corresponding peak loads are depicted in Figure 4-24. All parameters remain consistent across these samples. Perhaps, the rising trend is attributed to cucumbers with larger diameters distributing the applied force over a broader surface. Conversely, cucumbers with smaller diameters experience higher pressure, leading to earlier instances of damage.



(a)

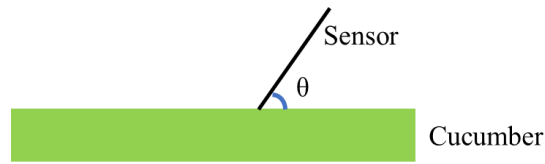


(b)

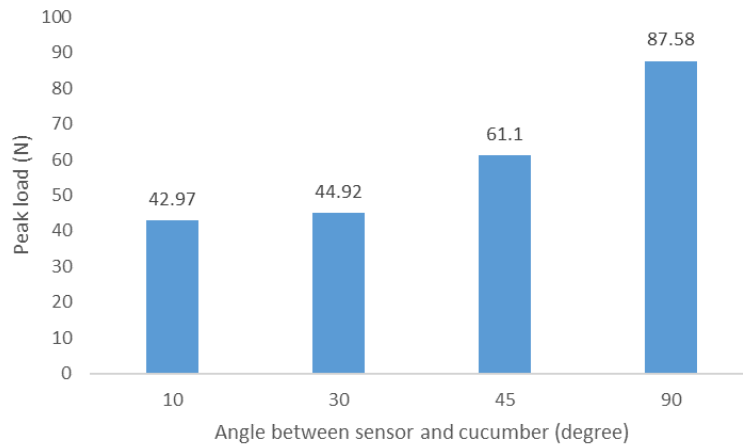


Figure 4-24. a. The direction of applying force, and b. The effect of diameter on peak load

In the other test, the influence of force direction on peak load is investigated. Within each of the three samples, four segments are generated, and the pressure sensor applies pressure at angles of 10, 30, 45, and 90 degrees. Subsequently, the graph is plotted as depicted in Figure 4-25. Damaging the cucumbers appears to be more pronounced when force is applied perpendicular to them, as opposed to when the force is applied more parallel to the cucumber axes. In other words, the perpendicular component of the force is what causes damage.



(a)



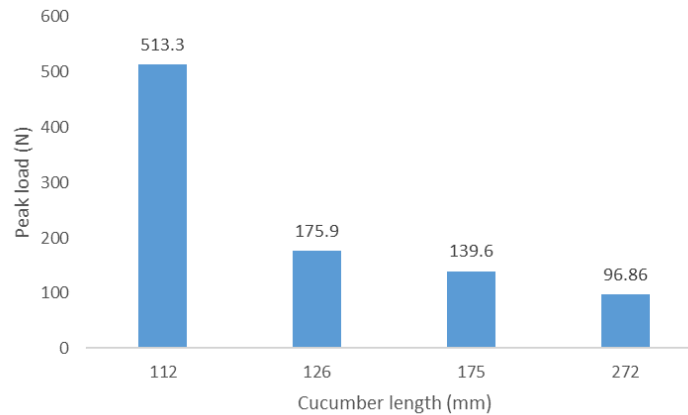
(b)

Figure 4-25. a. The direction of applying force, and b. The effect of angle on peak load

Impact of cucumber length is investigated. Four cucumbers are selected. The resulting graph is shown in Figure 4-26. The adjustment for the trend is that lengthy cucumbers would be affected by buckling more than the short ones. Thus, lengthy ones break sooner.



(a)



(b)

Figure 4-26. a. The direction of applying force, and b. Effect of cucumber length on peak load

#### 4.6. Cost analysis

The results of an analysis comparing the cost variances between traditional and automated harvesting is presented in this section. In this analysis, there are a couple of main assumptions. Firstly, it is assumed that the time required for a robot to harvest one cucumber is four times longer than the time needed for a human labourer to harvest the same cucumber. Secondly, it is assumed that a robot operates for 24 hours a day, whereas a labourer works for 6 hours a day. Based on these assumptions, it can be inferred that although a labourer works for fewer hours (6 hours) but at a speed four times faster than a robot, they can be effectively replaced by a robot operating for 24 hours, albeit at a speed four times slower than the labourer. Consequently, this analysis considers the replacement of 20 labourers with 20 robots.

Traditional cost themes are as follows and are summarized in Table 4-5 (all in CAD).

- Human labour (20 people) is considered for 250 days (50 weeks, 5 days each week), with 6 hours each day, at a minimum wage of \$16.55 per hour: \$2482K

- Insurance is approximately 2.2% of the overall wage (based on WSIB ON): \$55K
- Benefit and payroll tax is calculated as 1.5 times the overall wage: \$3723K
- Energy costs for robots are equated to the trolley cost associated with manual labour, which is considered to be zero.

Table 4-5. Cost analysis results in manual cucumber harvesting

Cost factor for five years	Cost CAD
Annual wage of harvesters (minimum: \$16.55 per hour)	\$2482K
Insurance (WSIB ON)	\$55 K
Benefit and payroll tax	\$3723 K
<b>Total</b>	<b>\$6261 K</b>

Parameters in calculating the automation harvesting cost are as follows and are summarized in Table 4-6.

- The total cost for 20 robotic systems is \$800K, in addition to the setup cost of \$500K.
- General equipment and system support (maintenance) over 5 years are calculated at \$125K, with consideration for a breakdown of 5% of robots.
- Decision-making algorithms cost 10 times the cost of the camera, totaling 100K.
- The vision system cost is \$10K.
- To mount the robot, the Ateago S4 mobile robot chassis costs \$220K.
- Human specialists, consisting of four people with an annual wage of \$80K each, sum up to \$1600K for five years.

- The analysis assumes that the robot becomes non-operational after 5 years because it becomes outdated or no longer useful due to technological advancements or changes in requirements.
- Overhead costs are factored into the robotic method at 20%, while the traditional method is assumed to have zero overhead.
- Energy costs for robots are equated to the trolley cost associated with manual labour, considered to be zero.

Table 4-6. Cost analysis results in automation of cucumber harvesting

Components	Component description	Total cost (CAD)
Setup and robot costs	Cost of buying robot, floor preparation, and training people Single arm with end effector	\$1300 K
Vision system	3D cameras (1 per robot)	\$10K
Decision making algorithms	Software costs Decision making for maintenance License fee IT support	\$100K
General equipment and system support (maintenance)	Highly skilled employees for maintenance, engineering, and software support, breakdown of 5% of robots	\$125 K
Specialists	Experienced workers	\$1600 K
Trolley	To mount the robot on it: Ateago S4 mobile robot chassis	\$220K

Total cost		\$3355 K
<b>Total cost including overhead (20%)</b>		<b>\$4026 k</b>

#### *4.7.OEE analysis*

Overall Equipment Effectiveness (OEE) is determined by multiplying availability, performance, and quality. OEE for both manual and automated cucumber harvesting methods are examined.

OEE parameters for manual harvesting are as follows.

- Availability: Workers are unable to work for the entire 8 hours, with one hour of non-productive time accounted for. Thus, the availability is 87.5%.
- Performance: Calculated with an ideal cycle time of 100 cucumbers per hour, the average total output is 90 cucumbers over a 7-hour runtime. Therefore, the performance is 90%.
- Quality: Assuming 10% of cucumbers have low quality, the overall quality is considered to be 90%.

The resulting OEE for the manual method is obtained by multiplying availability, performance, and quality which would be 71%.

OEE parameters for automated harvesting are as follows.

- Availability: Accounting for a 5% daily damage rate to robots, the availability is considered to be 95%.
- Performance: The performance is evaluated at 99%.
- Quality: Similar to the manual method, 10% of cucumbers are assumed to have low quality, resulting in an overall quality of 90%.

The final OEE for the automated method is obtained by multiplying availability, performance, and quality which would be 85%.

#### *4.8. Summary*

Here are some summaries of the results.

- For both cucumber bounding box and keypoints detections, YOLOL affirmed as the superior model as confirmed by F1-confidence curve and the fact that there is no false positive when detecting with YOLOL.
- Near-real-time detection in YOLON reveals misses, possibly attributed to the swift video recording pace.
- During the robot's harvesting trajectory, successful trajectory and cutting without accidents are observed.
- In RGB analysis, cucumber values consistently rank lower than stem ends, vines, and leaves. Vines exhibit the highest RGB values between plant components. The B value shows ineffectiveness for detection purposes because plant components share the similar value in B.
- Analysis of cucumber properties reveals that samples with higher G values can tolerate more force. Moreover, a straighter cucumber withstands greater axial loads, and increasing diameter correlates with increased peak load tolerance. An increase in length correlates with a decrease in peak axial load. However, more samples and tests are needed to verify this. The system design should consider the worst-case scenario to ensure that no damage occurs to the surface of cucumbers during harvesting.
- ImageJ and Fiji exhibit successful background removal and successful boundaries detection of plant components.
- RoboFlow platform shows accurate cucumber bounding box identification.
- Geometry analysis in MATLAB aligns well with real cucumber shapes, regardless of curve fitting order, as long as it is not linear fitting.
- Python script for manipulation of RGB-XYZ data shows promise in filtering pixels based on input RGB intervals and sorting them based on Z value.

- Cost analysis anticipates a minimum 35% reduction in cucumber harvesting costs over a 5-year period with the proposed automation.
- OEE demonstrates improvement from 71% to 85% after shifting from manual harvesting to automation.

## 5. CONCLUSION AND FUTURE

The conclusion of this study is as follows.

1. Proposed harvesting framework is promising because:
  - Successful harvesting framework (like camera installations and cutting blades)
  - Successful near-real-time detection using YOLO
  - Successful robot trajectory with minor contact with plant
2. Presented false negatives in detection may be mitigated by dynamic camera movements.
3. Detection accuracy is not conclusive for final cutting point at this stage.
4. Cucumber characteristics influence peak load tolerance: increasing G value, curvature, and length decreases the peak force. However, increasing diameter and sensor angle rises the peak load.
5. Geometry analysis shows a good curve fitting.
6. Cost analysis reveal potential improvements.

For the future there are some suggestions:

1. Test under various lighting conditions.
2. Manage directly raw RGB-XYZ data from 3D camera for cucumber shape detection.
3. Cuts & grips cucumbers simultaneously.
4. Study on cost analysis in more depth.
5. Send a command to the client (robot) automatically.
6. Collect data on greenhouse environment for modeling.



## REFERENCES

- [1] [https://publications.gc.ca/collections/collection\\_2009/agr/A118-10-15-2006E.pdf](https://publications.gc.ca/collections/collection_2009/agr/A118-10-15-2006E.pdf), January 19, 2024.
- [2] Statistical Overview of the Canadian Greenhouse Vegetable Industry, 2018, Prepared by: Crops and Horticulture Division, Agriculture and Agri-Food Canada, December 2019, January 19, 2024.
- [3] N S M Nawik et al 2015 IOP Conf. Ser.: Mater. Sci. Eng. 100 012045, 10.1088/1757-899X/100/1/012045
- [4] Jing, W.; Leqi, W.; Yanling, H.; Yun, Z.; Ruyan, Z. On Combining DeepSnake and Global Saliency for Detection of Orchard Apples. *Appl. Sci.* 2021, 11, 6269. <https://doi.org/10.3390/app11146269>
- [5] Zheng, B.; Sun, G.; Meng, Z.; Nan, R. Vegetable Size Measurement Based on Stereo Camera and Keypoints Detection. *Sensors* 2022, 22, 1617. <https://doi.org/10.3390/s22041617>
- [6] Jordi Gené-Mola, Verónica Vilaplana, Joan R. Rosell-Polo, Josep-Ramon Morros, Javier Ruiz-Hidalgo, Eduard Gregorio, Multi-modal deep learning for Fuji apple detection using RGB-D cameras and their radiometric capabilities, *Computers and Electronics in Agriculture*, 162, July 2019, Pages 689-698, <https://doi.org/10.1016/j.compag.2019.05.016>
- [7] Kamran Kheiralipour, Abbas Pormah, Introducing new shape features for classification of cucumber fruit based on image processing technique and artificial neural networks, *Journal of food process engineering*, 40, Issue6, <https://doi.org/10.1111/jfpe.12558>
- [8] Md Khurram Monir Rabby, Brinta Chowdhury, and Jung H. Kim 2A Modified Canny Edge Detection Algorithm for Fruit Detection & Classification, *10th International Conference on Electrical and Computer Engineering*, 20-22 December, 2018, Dhaka, Bangladesh
- [9] Xiaoyang Liu, Dean Zhao, Weikuan Jia, Wei Ji, Yueping Sun, A Detection Method for Apple Fruits Based on Colour and Shape Features, *Computer Science*, 7, 67923 – 67933, <https://doi.org/10.1109/ACCESS.2019.2918313>

- [10] Shuqin Tu, Jing Pang, Haofeng Liu, Nan Zhuang, Yong Chen, Chan Zheng, Hua Wan, Yueju Xue, Passion fruit detection and counting based on multiple scale faster R-CNN using RGB-D images, *Precision Agriculture* (2020) 21, 1072–1091, <https://doi.org/10.1007/s11119-020-09709-3>
- [11] Dadang Iskandar, Marjuki, Classification of Melinjo Fruit Levels Using Skin Colour Detection With RGB and HSV, *Journal of Applied Engineering and Technological Science*, 4(1) 2022, 123-130
- [12] B. J. McGuinness, Mike D. Duke, Kit C. Au, Hin S. Lim, Field factory for the automated harvesting of forestry tree stock, *Biosystems Engineering*, Volume 227, 2023, Pages 52-67, <https://doi.org/10.1016/j.biosystemseng.2023.01.003>
- [13] T. Yoshida, Y. Onishi, T. Kawahara, and T. Fukao, Automated harvesting by a dual-arm fruit harvesting robot, *ROBOMECH Journal* (2022) 9:19, <https://doi.org/10.1186/s40648-022-00233-9>
- [14] M N Shaprov, A V Sedov, O P Sedova, M V Ulyanov and A V Gurba, IOP Conf. Series: *Earth and Environmental Science* 965 (2022) 012057, IOP Publishing, doi:10.1088/1755-1315/965/1/012057
- [15] P. Eizentals, K. Oka, 3D pose estimation of green pepper fruit for automated harvesting, *Computers and Electronics in Agriculture* 128 (2016) 127–140, <http://dx.doi.org/10.1016/j.compag.2016.08.024>
- [16] Young K. Chang, Qamar Zaman, Aitazaz A. Farooque, Arnold W. Schumann, David C. Percival, An automated yield monitoring system II for commercial wild blueberry double-head harvester, *Computers and Electronics in Agriculture*, 2012, **81** (97-103), <https://doi-org.ledproxy2.uwindsor.ca/10.1016/j.compag.2011.11.012>
- [17] J. R. Davidson, A. Silwal, C. J. Hohimer, M. Karkee, C. Mo and Q. Zhang, "Proof-of-concept of a robotic apple harvester," 2016 IEEE/RSJ International Conference on Intelligent Robots and Systems (IROS), Daejeon, Korea (South), 2016, pp. 634-639, doi: 10.1109/IROS.2016.7759119.
- [18] [https://www.universal-robots.com/products/ur3-robot/?utm\\_source=Bing&utm\\_medium=cpc&utm\\_cja=Demo&utm\\_leadsource=Paid%20Search](https://www.universal-robots.com/products/ur3-robot/?utm_source=Bing&utm_medium=cpc&utm_cja=Demo&utm_leadsource=Paid%20Search)

&utm\_campaign=HQ\_CA\_Always-  
On2021&utm\_content=textad&utm\_term=ur3e&msclkid=485fae7f834a1ac6d8b1cbc6205189a8,  
January 19, 2024.

[19] Intel website: <https://www.intelrealsense.com/depth-camera-d435if/>, January 19, 2024

[20] <https://github.com/ultralytics/ultralytics>, January 19, 2024

[21] Grabcad website: <https://grabcad.com/>, January 19, 2024

[22] <https://www.cvat.ai/>, January 19, 2024

[23] <https://docs.ultralytics.com/tasks/pose/> January 19, 2024

## APPENDICES

### *APPENDIX A. UR3e specifications*

The UR3e specifications are mentioned as Figure A-1. More information regarding technical specification of UR3e robot on reference [18].

<b>UR3e</b>		
<b>Specification</b>		
Payload	3 kg (6.6 lbs)	
Reach	500 mm (19.7 in)	
Degrees of freedom	6 rotating joints	
Programming	12 inch touchscreen with polyscope graphical user interface	
<b>Performance</b>		
Power, Consumption, Maximum Average	300 W	
Power, Consumption, Typical with moderate settings (approximate)	100 W	
Safety	17 configurable safety functions	
Certifications	EN ISO 13849-1, PLd Category 3, and EN ISO 10218-1	
Force Sensing, Tool Flange	Force, x-y-z	Torque, x-y-z
Range	30.0 N	10.0 Nm
Precision	2.0 N	0.1 Nm
Accuracy	3.5 N	0.1 Nm
<b>Movement</b>		
Pose Repeatability per ISO 9283	± 0.03 mm	
Axis movement	Working range	Maximum speed
Base	± 360°	± 180°/s
Shoulder	± 360°	± 180°/s
Elbow	± 360°	± 180°/s
Wrist 1	± 360°	± 360°/s
Wrist 2	± 360°	± 360°/s
Wrist 3	Infinite	± 360°/s

Figure A-1. UR3e specifications

## ***APPENDIX B. D435if: Intel RealSense software and specifications***

By combining LiDAR and stereo depth technology, these cameras generate point clouds based on time-of-flight sensors, providing both colour and geometry information about the scene.

Due to their ability to capture depth information, 3D cameras are valuable for accurately determining positions. Several studies utilize 3D cameras from manufacturers like Microsoft and Canon.

The process encompasses several steps: estimating extrinsic parameters, rectifying left and right images, calculating disparities to obtain the data cloud, and measuring object distances. To precisely pinpoint positions, the use of 3D cameras is imperative, given their ability to provide depth data. Various studies employ a diverse array of 3D cameras from manufacturers such as Microsoft and Canon.

A thorough examination of the Intel RealSense 3D Webcam D435if is conducted as it is utilized in this study. Figure B-1 showcases its physical components. The information presented here is sourced from Intel's official website.

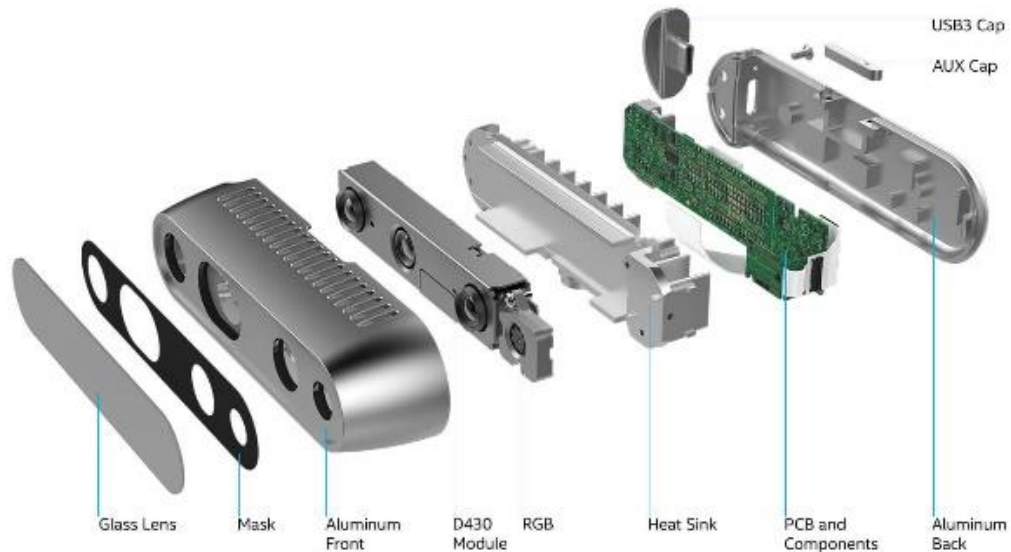


*Figure B-1. Intel RealSense 3D Webcam D435if physical components*

Intel produces 3D cameras under the RealSense brand, and the D4 series, including models like D435 and D455, incorporates LiDAR and stereo depth technologies. Although each series has distinct characteristics, they are commonly utilized in machine-vision-based

devices. The D435if operates on a USB 5V power supply, consuming approximately 1.5 W. Below, the capabilities of this specific 3D camera are explored in detail.

Intel RealSense 3D Webcam D435if possesses the distinctive capability to capture colour information and XYZ data simultaneously. Moreover, module data can be extracted from this camera. In this context, depth refers to the distance between each image point and the camera. Utilizing time-of-flight sensors, this camera acquires depth data, facilitating the generation of a point cloud for reconstructing the scene's geometry. Additionally, with its RGB cameras, the Intel RealSense 3D Webcam D435if can furnish colour information for images as shown in Figure B-2.



Figure B-2. An illustrative example of the D435if's output.

An overview of the camera key specifications is presented in Table B-1.

Table B-1. An overview of the key camera specifications, highlighting the key parameters.

Parameter	Range
<b>Ideal range</b>	<b>0.3 m to 3 m</b>
<b>Depth Accuracy</b>	<b>&lt;2% at 2 m</b>
Depth Field of View (FOV):	: 87° × 58° [Angular vertical and horizontal measurements]
Depth output resolution	Up to 1280 × 720 [number of pixels]
<b>RGB frame resolution</b>	<b>1920 × 1080</b>
RGB sensor FOV (H × V)	69° × 42°
<b>RGB sensor resolution</b>	<b>2 MP</b>
<b>Length × Depth × Height</b>	<b>90 mm × 25 mm × 25 mm</b>

### ***APPENDIX C. Camera setup and calibration***

Dynamic Calibrator software is used for calibrating D435 series cameras. As depicted in Figure C-1, initially, the camera is connected to a laptop, and the RealSense software is launched.



*Figure C-1. Camera setup*

Subsequently, a transition to 2D mode is performed to enable simultaneous access to RGB and 3D modes, as illustrated in Figure C-2. The upper right side corresponds to the 3D mode, while the lower right side represents the RGB mode. The left side is associated with the Inertial Measurement Unit (IMU) and the camera's position, which is a specific feature in the D435if camera.

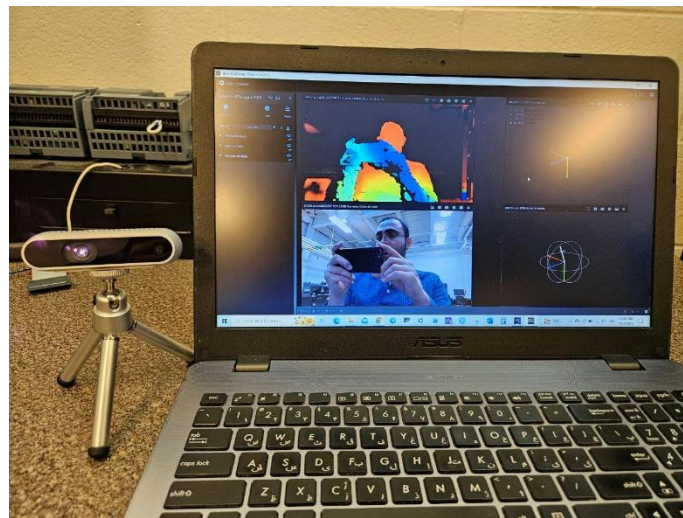


*Figure C-2. Switching different modes in camera*

There is a document available on the Intel website titled "Intel RealSense Calibration Print Target," which is shown in Figure C-3.

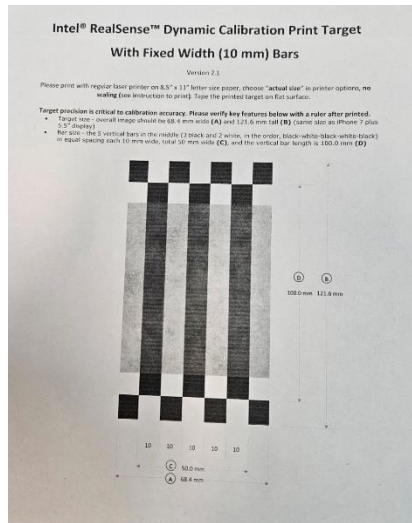


Figure C-3. Dynamic calibration print target

The next step involves running the Intel RealSense Dynamic Calibrator software. For this study, version 2.13.1 of the software is utilized. As illustrated, the Intel RealSense Calibration print target should be printed. The page needs to be positioned in various orientations, directions, and distances from the camera to calibrate the XYZ mode, as depicted in Figure C-4.

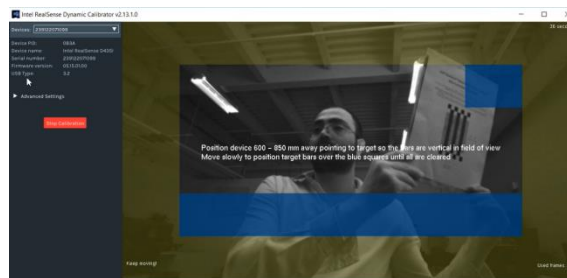
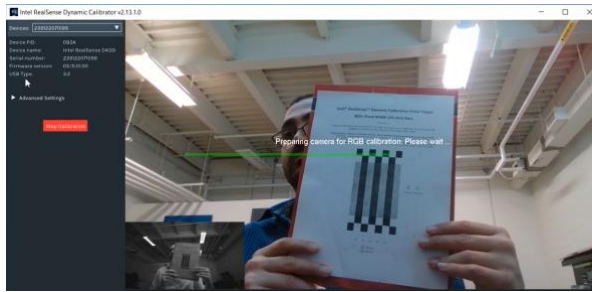


Figure C-4. The process of x, y, and z calibration

The process for calibrating the RGB mode is the same as the XYZ mode calibration. Following the XYZ calibration, the RGB calibration interface appears, and the printed page should be moved in different directions and angles, as depicted in Figure C-5.





*Figure C-5. RGB calibration and different positions that dynamic calibration print target should be placed*

#### ***APPENDIX D. Managing RGB-XYZ data in Python***

The target is the position of the stem end, determined by applying mathematical processes to the identified RGB values. Initially, the centre of the cucumber is determined using the following equations:

$$Y_{centre} = \sum_{i=1}^n y_i / n$$

$$X_{centre} = \sum_{i=1}^n x_i / n$$

Then, the length and width of the cucumber is calculated using the following equations. The maximum x (y) represents the average of the 1000 maximum x (y) values in a group.

$$\text{Length of cucumbercentre} = x_{max} - x_{min}$$

$$\text{Width of cucumbercentre} = y_{max} - y_{min}$$

Finally, the position of stem end is;

$$X \text{ stem end} = x_{centre} + \text{Length} / 2 + \epsilon$$

$$Y \text{ stem end} = Y_{centre}$$

## APPENDIX E. Client interfaces

Generally, the interface can be accomplished using six methods, as shown in Figure E-1 each with its specific criteria, equipment, and methods. The following line provides further insight into them.

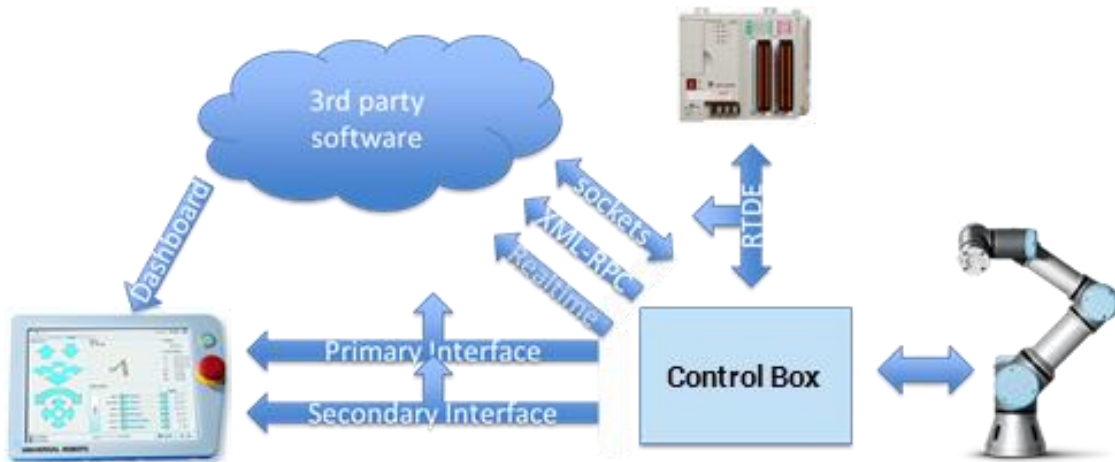


Figure E-1. All interfaces provided by UR companies

**Primary/Secondary interfaces:** According to the company's information, UR controllers serve as the central intelligence for these robots, overseeing both motion control and communication with external servers. The controller consistently monitors the robot's position and status, relaying this real-time information to external devices. The programming language employed in these robots is URScript, through which external devices transmit commands. Upon receiving a URScript code, the robot executes the corresponding command, essentially allowing the UR controller to share the robot's current state information and respond to URScript inputs from external devices, such as an image processing unit.

**Real-time interfaces:** It functions similarly to a primary and secondary interface, differing only in the transition and update rates.

**Dashboard server interfaces:** The Universal Robot company offers users the capability to transmit straightforward commands, such as pause and load, from an external source. This feature is facilitated through a dashboard server, with the robot seamlessly receiving these commands via TCP/IP socket communication.

Socket communication interfaces: Data transfer occurs through socket communication between the robot and external devices. In this communication setup, the robot functions as the client, while the external device operates in the role of the server.

Extensible Markup Language Remote Procedure Call (XML-RPC) interfaces: URScript is limited in performing complex calculations. To address this, Remote Procedure Call (RPC) utilizes XML language to facilitate data transfer between programs via sockets. Through XML-RPC, integration with other software packages becomes possible, enhancing the capabilities of URScript.

### ***APPENDIX F. Container***

Designing a container for collecting cucumbers during automated harvesting is a crucial aspect of the process. The container should meet some requirements. Firstly, it should have sufficient capacity to hold a significant quantity of cucumbers without overflowing, ensuring it can effectively accommodate the harvested produce. Secondly, the container's structure needs to be stable and capable of withstanding the weight and impact of falling cucumbers. Durability and resistance to damage are essential attributes. The container should be designed for easy access, allowing for the convenient removal of the collected cucumbers. Additionally, it should prevent cucumbers from rolling out or being damaged during collection, which may involve incorporating a secure cover to ensure the cucumbers remain protected and contained. Finally, in the future, a system should be developed to detect when containers are full. Another approach involves determining the maximum number of cucumbers in each greenhouse row. Then, at the end of each row, the robot would dump the full container to prepare for the next row. Data collection to determine the maximum cucumber count per row in the farm is essential.

### **APPENDIX G. Geometry analysis**

The raw XYZ data got from 3D camera for each cucumber sample are presented in Tables G-1 to G-5.

*Table G-1. The output data gained from 3D camera for the borders of the initial cucumber sample*

Section	Vector	X (m)	Y (m)	Z (m)	$\Delta y$ (cucumber diameter)
Section 1	Vector 1	-0.046	0.009	0.207	31 mm
	Vector 2	-0.047	0.040	0.205	
Section 2	Vector 1	-0.036	0.016	0.208	29 mm
	Vector 2	-0.036	0.043	0.203	
Section 3	Vector 1	-0.024	0.022	0.209	31 mm
	Vector 2	-0.025	0.053	0.210	
Section 4	Vector 1	-0.015	0.023	0.208	33 mm
	Vector 2	-0.015	0.056	0.211	
Section 5	Vector 1	-0.006	0.012	0.211	37 mm
	Vector 2	-0.005	0.049	0.208	
Section 6	Vector 1	0.001	0.005	0.210	35 mm
	Vector 2	0.001	0.040	0.206	
Section 7	Vector 1	0.006	-0.004	0.212	42 mm
	Vector 2	0.007	0.038	0.208	

Table G-2. The data obtained from the 3D camera for the boundaries of the second cucumber sample

Section	Vector	X (m)	Y (m)	Z (m)	$\Delta y$ (cucumber diameter)
Section 1	Vector 1	-0.088	0.033	0.209	18 mm
	Vector 2	-0.089	0.051	0.211	
Section 2	Vector 1	-0.072	0.030	0.209	20 mm
	Vector 2	-0.072	0.050	0.210	
Section 3	Vector 1	-0.057	0.026	0.211	28 mm
	Vector 2	-0.056	0.054	0.213	
Section 4	Vector 1	-0.036	0.027	0.211	25 mm
	Vector 2	-0.035	0.052	0.215	
Section 5	Vector 1	-0.018	0.025	0.214	28 mm
	Vector 2	-0.018	0.053	0.219	
Section 6	Vector 1	-0.006	0.027	0.213	24 mm
	Vector 2	-0.006	0.051	0.221	
Section 7	Vector 1	0.006	0.024	0.216	23 mm
	Vector 2	0.007	0.047	0.217	

Table G-3. Data acquired from the 3D camera for the edges of the third cucumber sample

Section	Vector	X (m)	Y (m)	Z (m)	$\Delta y$ (cucumber diameter)
Section 1	Vector 1	-0.048	0.029	0.232	17 mm
	Vector 2	-0.048	0.046	0.227	
Section 2	Vector 1	-0.035	0.024	0.229	14 mm
	Vector 2	-0.036	0.038	0.225	
Section 3	Vector 1	-0.025	0.020	0.235	13 mm
	Vector 2	-0.025	0.033	0.223	
Section 4	Vector 1	-0.004	0.018	0.237	12 mm
	Vector 2	-0.004	0.030	0.223	
Section 5	Vector 1	0.017	0.023	0.240	13 mm
	Vector 2	0.016	0.036	0.223	
Section 6	Vector 1	0.030	0.031	0.225	13 mm
	Vector 2	0.030	0.044	0.230	
Section 7	Vector 1	0.040	0.036	0.227	9 mm
	Vector 2	0.039	0.045	0.228	



Table G-4. Information obtained from the 3D camera for the boundaries of the fourth cucumber sample

Section	Vector	X (m)	Y (m)	Z (m)	$\Delta y$ (cucumber diameter)
Section 1	Vector 1	-0.048	0.017	0.207	26 mm
	Vector 2	-0.047	0.043	0.203	
Section 2	Vector 1	-0.028	0.019	0.206	26 mm
	Vector 2	-0.028	0.045	0.202	
Section 3	Vector 1	-0.012	0.023	0.203	27 mm
	Vector 2	-0.012	0.050	0.204	
Section 4	Vector 1	-0.003	0.020	0.205	29 mm
	Vector 2	-0.001	0.049	0.205	
Section 5	Vector 1	0.015	0.019	0.203	28 mm
	Vector 2	0.015	0.047	0.202	
Section 6	Vector 1	0.029	0.018	0.202	25 mm
	Vector 2	0.029	0.043	0.202	
Section 7	Vector 1	0.041	0.016	0.206	22 mm
	Vector 2	0.041	0.038	0.203	

Table G-5. Data acquired from the 3D camera for the edges of the fifth cucumber sample

Section	Vector	X (m)	Y (m)	Z (m)	$\Delta y$ (cucumber diameter)
Section 1	Vector 1	-0.049	0.035	0.216	13 mm
	Vector 2	-0.049	0.048	0.218	
Section 2	Vector 1	-0.044	0.029	0.219	15 mm
	Vector 2	-0.043	0.044	0.216	
Section 3	Vector 1	-0.031	0.025	0.220	15 mm
	Vector 2	-0.030	0.040	0.219	
Section 4	Vector 1	-0.018	0.022	0.223	14 mm
	Vector 2	-0.018	0.036	0.220	
Section 5	Vector 1	-0.007	0.025	0.222	15 mm
	Vector 2	-0.007	0.040	0.222	
Section 6	Vector 1	0.003	0.027	0.224	14 mm
	Vector 2	0.004	0.041	0.222	
Section 7	Vector 1	0.010	0.033	0.223	13 mm
	Vector 2	0.009	0.046	0.225	

## ***APPENDIX H. Detailed data collection plan***

Having an understanding of the shapes and colours of all plant components and the physical environment within the greenhouse can help further process modeling and image processing.

Recommended data collection themes for cucumber appearance are length, diameter, and geometry. Themes for stem end appearance are length, diameter, geometry, and stem end angle with cucumber. Data collection themes for vines/stalk appearance is only diameter. Suggested themes for leaves appearance are length and shape. Data collection on RGBs of cucumber, stem end, vines, leaves, blossom end is recommended. Data collection on blossom end appearance includes length, diameter, geometry, and blossom end angle with cucumber. Distribution profile of cucumbers and angle of stem end and vines are also two other themes. Data collection themes for greenhouse environment includes growth height from ground, lower height, upper height, and consecutive pods distance. Themes for greenhouse environment are general layout, pod and cucumber distance, gap in each row, length of each row, parallel rails distance, rail width, cucumber and frame distance, harvesting cycle (growth rate), and number of pods in each row.

For each mentioned theme, information on definition, data collection methods, the instruments used, sample frequency, data type, data sources, limitations, anticipated time requirements, minimum number of collectors, sample size, and sketches of the parameters are needed, which are elaborated as follows.




First, cucumber appearance is a crucial factor to consider because the image processing unit needs to recognize its external features for detection. There are four main parameters related to cucumber appearance, and they are elaborated in the rest of the passage.

The details for data collection on cucumber length are provided in Table H-1.

*Table H-1. Data collection plan for length and diameter of cucumber*

	<b>Cucumber length (mm)</b>	<b>Cucumber D average (mm)</b>	<b>Cucumber D max (mm)</b>
--	---------------------------------	------------------------------------	--------------------------------

Definition	Straight distance between stem end and blossom end	Average Diameter of cucumber	Max Diameter of cucumber
How? Methods	Manual measurement	Manual measurement	Manual measurement
What instruments?	Caliper	Caliper	Caliper
Why? Which research questions will be addressed?	Shape recognition	Shape recognition	Shape recognition
Sample frequency: How much/many data	Random 30 cucumbers	Random 30 cucumbers	Random 30 cucumbers
Data type (continuous or discrete, quantitative or qualitative)	Discrete, quantitative	Discrete, quantitative	Discrete, quantitative
Data sources	Market, Commercial greenhouses	Market, Commercial greenhouses	Market, Commercial greenhouses
Limitations	N/A	N/A	N/A
Predicted needed time (minutes)	60	150	150
Minimum people needed as collectors	1	1	1
How often the data is collected?	Multiple sessions	Multiple sessions	Multiple sessions

Sample size: the number of data points collected per sample	2	5	5
When the data are collected?	TBD	TBD	TBD
Day or night, What time?	TBD	TBD	TBD
Sunlight condition (very cloudy, cloudy, sunny, strong sunlight)	TBD	TBD	TBD
Distance between camera and pod	TBD	TBD	TBD
Sketch of theme			

The details for data collection on cucumber's geometry are provided in Table H-2.

*Table H-2. Data collection plan for geometry of cucumber*

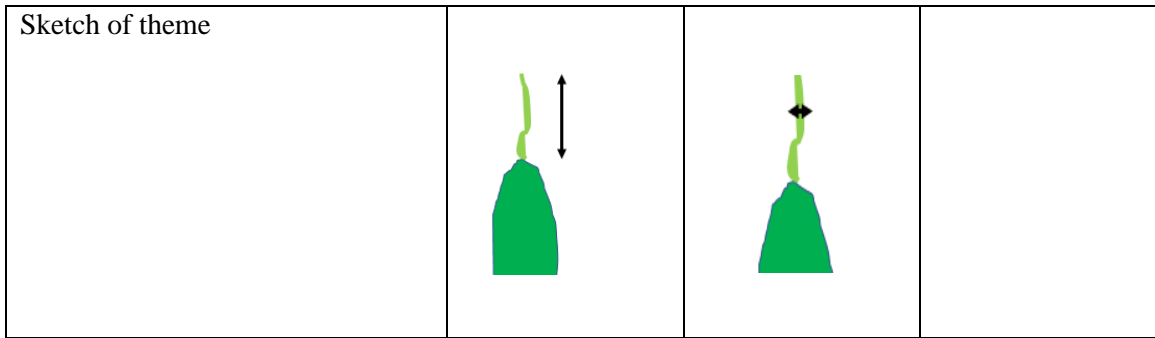
	<b>Cucumber Geometry</b>
Definition	General shape of cucumbers. One example is bell-shape cucumber

How? Methods	Visual observation
What instruments?	N/A
Why? Which research questions will be addressed?	shape recognition
Sample frequency: How much/many data	Random 30 cucumbers
Data type (continuous or discrete, quantitative or qualitative)	Discrete, quantitative
Data sources	Market, Commercial greenhouses
Limitations	N/A
Predicted needed time (minutes)	30
Minimum people needed as collectors	1
How often the data is collected?	Multiple sessions
Sample size: the number of data points collected per sample	1
When the data are collected?	TBD
Day or night, What time?	TBD
Sunlight condition (very cloudy, cloudy, sunny, strong sunlight)	TBD
Distance between camera and pod	TBD
Sketch of theme	N/A

The details for data collection on length of stem end are provided in Table H-3.

*Table H-3. Data collection plan for stem end's length and diameter*

	<b>Stem end length (mm)</b>	<b>Stem end D mean (mm)</b>	<b>Stem end D max (mm)</b>
Definition	The length of stem end	Average Diameter of stem end	Max Diameter of stem end
How? Methods	Manual measurement	Manual measurement	Manual measurement
What instruments?	Caliper	Caliper	Caliper
Why? Which research questions will be addressed?	Shape recognition	Shape recognition	Shape recognition
Sample frequency: How much/many data	Random 30 leaves	Random 30 stem ends	Random 30 stem ends
Data type (continuous or discrete, quantitative or qualitative)	Discrete, quantitative	Discrete, quantitative	Discrete, quantitative
Data sources	Market, Commercial greenhouses	Market, Commercial greenhouses	Market, Commercial greenhouses
Limitations	N/A	N/A	N/A
Predicted needed time (minutes)	60	150	60
Minimum people needed as collectors	1	1	1
How often the data is collected?	Multiple sessions	Multiple sessions	Multiple sessions
Sample size: the number of data points collected per sample	2	5	2
When the data are collected?	TBD	TBD	TBD
Day or night, What time?	TBD	TBD	TBD
Sunlight condition (very cloudy, cloudy, sunny, strong sunlight)	TBD	TBD	TBD
Distance between camera and pod	TBD	TBD	TBD




The details for data collection on geometry of cucumber are provided in Table H-4.

*Table H-4. Data collection plan for geometry of stem end and its angle with cucumber*

	<b>Stem end geometry</b>	<b>Stem end angle with cucumber</b>
Definition	The profile of stem end where it reaches to cucumber	the angle between cucumber and stem end
How? Methods	Taking pictures and interpreting the geometries	Manual measurement
What instruments?	Camera, geometry analysis using math	protractor
Why? Which research questions will be addressed?	shape recognition	shape recognition
Sample frequency: How much/many data	Random 150 shapes	Random 150 shapes
Data type (continuous or discrete, quantitative or qualitative)	Continuous, qualitative	Continuous, qualitative
Data sources	Market, Commercial greenhouses	Commercial greenhouses
Limitations	N/A	N/A
Predicted needed time (minutes)	30	30
Minimum people needed as collectors	1	2
How often the data is collected?	Multiple sessions	Multiple sessions
Sample size: the number of data points collected per sample	1	2
When the data are collected?	TBD	TBD

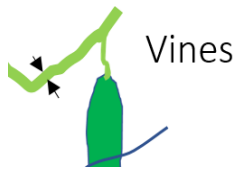


Day or night, What time?	TBD	TBD
Sunlight condition (very cloudy, cloudy, sunny, strong sunlight)	TBD	TBD
Distance between camera and pod	TBD	TBD
Sketch of theme	N/A	

The details for data collection on Dmean and Dmax of vines are provided in Table H-5.

Table H-5. Data collection plan for diameters of vine

	<b>Vines/stalk D mean (mm)</b>	<b>Vines/stalk D max (mm)</b>
Definition	Average Diameter of Vines/stalk	Max Diameter of vines/stalk
How? Methods	Manual measurement	Manual measurement
What instruments?	Caliper	Caliper
Why? Which research questions will be addressed?	Shape recognition	Shape recognition
Sample frequency: How much/many data	Random 30 samples	
Data type (continuous or discrete, quantitative or qualitative)	Discrete, quantitative	Discrete, quantitative
Data sources	Commercial greenhouses	Commercial greenhouses
Limitations	N/A	N/A

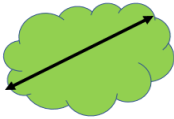
Predicted needed time (minutes)	150	150
Minimum people needed as collectors	1	1
How often the data is collected?	One session	One session
Sample size: the number of data points collected per sample	5	5
When the data are collected?	TBD	TBD
Day or night, What time?	TBD	TBD
Sunlight condition (very cloudy, cloudy, sunny, strong sunlight)	TBD	TBD
Distance between camera and pod	TBD	TBD
Sketch of theme		

The details for data collection on length of leaf are provided in Table H-6.

*Table H-6. Data collection plan for length and shape of leaf*

	<b>Leaf length (mm)</b>	<b>Leaf shape</b>

Definition	maximum distance between two points in one leave	General shape of leaves like 5 lobed
How? Methods	Manual measurement	Manual measurement
What instruments?	Caliper	N/A
Why? Which research questions will be addressed?	Shape recognition	Shape recognition
Sample frequency: How much/many data	Random 30 leaves	Random 30 leaves
Data type (continuous or discrete, quantitative or qualitative)	Discrete, quantitative	Discrete, quantitative
Data sources	Commercial greenhouses	Commercial greenhouses
Limitations	N/A	N/A
Predicted needed time (minutes)	60	30
Minimum people needed as collectors	1	1
How often the data is collected?	One session	One session
Sample size: the number of data points collected per sample	2	1
When the data are collected?	TBD	TBD
Day or night, What time?	TBD	TBD

Sunlight condition (very cloudy, cloudy, sunny, strong sunlight)	TBD	TBD
Distance between camera and pod	TBD	TBD
Sketch of theme		N/A

The details for data collection on distribution profile are provided in Table H-7.

*Table H-7. Data collection plan for distribution profile*

	<b>Distribution profile</b>
Definition	How cucumbers are distributed around the vines
How? Methods	visual observation
What instruments?	N/A
Why? Which research questions will be addressed?	The locations that the robot stops to take pictures
Sample frequency: How much/many data	Random 30 pods
Data type (continuous or discrete, quantitative or qualitative)	Discrete, quantitative
Data sources	Commercial greenhouses
Limitations	N/A
Predicted needed time (minutes)	60
Minimum people needed as collectors	1
How often the data is collected?	One session

Sample size: the number of data points collected per sample	1
When the data are collected?	TBD
Day or night, What time?	TBD
Sunlight condition (very cloudy, cloudy, sunny, strong sunlight)	TBD
Distance between camera and pod	TBD
Sketch of theme	N/A

The details for data collection on RGBs of cucumber, stem end, vine, blossom end, and leaf are provided in Table H-8.

*Table H-8. Data collection plan for RGBs of cucumber, stem end, vine, blossom end, and leave*

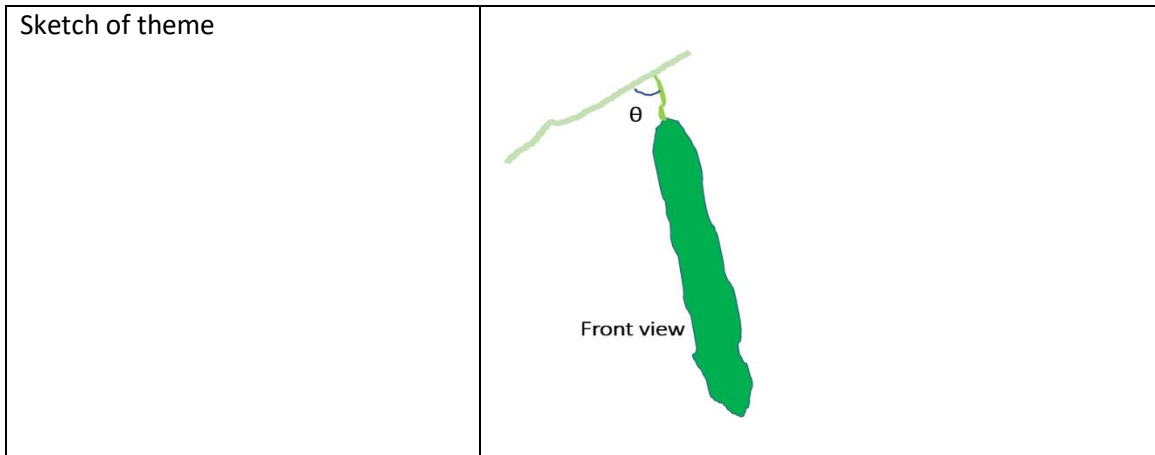
	<b>Cucumber RGB</b>	<b>Stem end RGB</b>	<b>Vines RGB</b>	<b>blossom end RGB</b>	<b>Leaves RGB</b>
Definition	Red, Green and Blue values of colour of cucumbers	Red, Green and Blue values of colour of stem ends	Red, Green and Blue values of colour of vines	Red, Green and Blue values of colour of blossom end	Red, Green and Blue values of colour of leaves
How? Methods	Take & analyze images	Take & analyze images	Take & analyze images	Take & analyze images	Take & analyze images
What instruments?	Camera & software	Camera & software	Camera & software	Camera & software	Camera & software
Why? Which research questions will be addressed?	Cucumber detection	stem end detection	Vines removal from image	cucumber detection	Leaves removal from image
Sample frequency: How much/many data	200	200	200	200	200
Data type (continuous or discrete, quantitative or qualitative)	discrete, quantitative	discrete, quantitative	discrete, quantitative	discrete, quantitative	discrete, quantitative

Data sources	Commercial greenhouses , Market	Commercial greenhouses , Market	Commercial greenhouses , Market	Commercial greenhouses, Market	Commercial greenhouses, Market
Limitations	N/A	N/A	N/A	N/A	N/A
Predicted time needed (minutes)	200	200	200	200	200
Minimum people needed as collectors	1	1	1	1	1
How often the data is collected?	One session	One session	One session	One session	One session
Sample size: the number of data points collected per sample	1	1	1	1	1
When the data are collected?	TBD	TBD	TBD	TBD	TBD
Day or night, What time?	TBD	TBD	TBD	TBD	TBD
Sunlight condition (very cloudy, cloudy, sunny, strong sunlight)	TBD	TBD	TBD	TBD	TBD
Distance between camera and pod	TBD	TBD	TBD	TBD	TBD
Sketch of theme	N/A	N/A	N/A	N/A	N/A

The details for data collection on angle between stem end and vine are provided in Table H-9.

Table H-9. Data collection plan for angle between stem end and vine

	<b>Angle between stem end and vines</b>
Definition	In plant, the stem end of each cucumber has an angle with its vine when looking at front view
How? Methods	Manual measurement
What instruments?	protractor
Why? Which research questions will be addressed?	Stem end detection
Sample frequency: How much/many data	50
Data type (continuous or discrete, quantitative or qualitative)	Discrete, quantitative
Data sources	Commercial greenhouses
Limitations	N/A
Predicted needed time (minutes)	50
Minimum people needed as collectors	1
How often the data is collected?	one session
Sample size: the number of data points collected per sample	1
When the data are collected?	TBD
Day or night, What time?	TBD
Sunlight condition (very cloudy, cloudy, sunny, strong sunlight)	TBD
Distance between camera and pod	TBD



The details for data collection on lower/upper height growth from ground are provided in Table H-10.

*Table H-10. Data collection plan for lower/upper height growth from ground*

	<b>Lower (upper) height (m)</b>
Definition	Distance between ground and the lowest (highest) cucumber's stem end
How? Methods	Manual measurement
What instruments?	measuring tape
Why? Which research questions will be addressed?	Finding: 1. Needed acutation of robot 2. Robot height
Sample frequency: How much/many data	Random 50 pods
Data type (continuous or discrete, quantitative or qualitative)	Discrete, quantitative
Data sources	Commercial greenhouses
Limitations	1. Measurement error (inaccurate tools, vertical error, etc.)
Predicted needed time (minutes)	100
Minimum people needed as collectors	1
How often the data is collected?	One session



Sample size: the number of data points collected per sample	2
When the data are collected?	TBD
Sketch of theme	<p>The diagram illustrates the measurement setup. At the top is a green cucumber. Below it is a blue horizontal bar labeled 'Horizontal frame'. Below the horizontal frame is another blue horizontal bar labeled 'ground'. A vertical double-headed arrow points from the bottom of the cucumber to the top of the horizontal frame, with the text 'Minimum distance between blossom end and metal frame' next to it.</p>

The details for data collection on consecutive pods distance are provided in Table H-11.

*Table H-11. Data collection plan for consecutive pods distance*

	<b>Consecutive pods distance (m)</b>
Definition	The distance between the centres of two consecutive pods in the same row
How? Methods	Manual measurement
What instruments?	measuring tape
Why? Which research questions will be addressed?	The horizontal step that the robot moves, then stops and starts taking picture in the vertical direction
Sample frequency: How much/many data	Random 5 samples
Data type (continuous or discrete, quantitative or qualitative)	Discrete, quantitative
Data sources	Commercial greenhouses
Limitations	1. Measurement error (vertical error, inaccurate tools, etc.)
Predicted needed time (minutes)	10

Minimum people needed as collectors	1
How often the data is collected?	One session
Sample size: the number of data points collected per sample	1
When the data are collected?	TBD

Some parameters to understand the greenhouse environment are as follows. The details for data collection plan are provided in Table H-12.

*Table H-12. Data collection plan for general layout, pod and cucumber distance and gap in each row*

	<b>General layout</b>	<b>Pod and cucumber distance</b>	<b>Gap in each row (m)</b>
Definition	Consecutive linear rows	Distance between a pod's bottom and the lowest cucumber from the same pod	The free distance in each row
How? Methods	Observation	Manual measurement	Manual measurement
What instruments?	N/A	measuring tape	measuring tape
Why? Which research questions will be addressed?	Robot design	Robot size	1. Robot size, 2. Accident avoidance
Sample frequency: How much/many data	N/A	Random 50 pods	Random 5 consecutive rows

Data type (continuous or discrete, quantitative or qualitative)	Qualitative	Discrete, quantitative	Discrete, quantitative
Data sources	Commercial greenhouses	Commercial greenhouses	Commercial greenhouses
Limitations	N/A	1. Measurement error (vertical error, inaccurate tools, etc.)	1. Measurement error (vertical error, inaccurate tools, etc.)
Predicted needed time (minutes)	10	100	10
Minimum people needed as collectors	1	1	1
How often the data is collected?	One session	One session	One session
Sample size: the number of data points collected per sample	N/A	2	1
When the data are collected?	TBD	TBD	TBD

Length of each row, parallel rails distance, and rail width

The details for data collection on length of each row are provided in Table H-13.

Table H-13. Data collection plan for length of each row, parallel rails distance, and rail width

	<b>Length of each row (m)</b>	<b>Parallel rails distance</b>	<b>Rail width (m)</b>
Definition	The rail length	The distance between two rails in one row	The width of one single rail
How? Methods	Manual measurement	Manual measurement	Manual measurement
What instruments?	measuring tape	measuring tape	Caliper
Why? Which research questions will be addressed?	Speed of robot	Robot width	Future improvement on the robot by elimination of harvesting trolley
Sample frequency: How much/many data	Random 2 rows	Random 3 rows	Random 3 rails
Data type (continuous or discrete, quantitative or qualitative)	Discrete, quantitative	Discrete, quantitative	Discrete, quantitative
Data sources	Commercial greenhouses	Commercial greenhouses	Commercial greenhouses
Limitations	1. measuring tape size, 2.	Measurement errors	N/A

	Measurement errors		
Predicted needed time (minutes)	10	10	10
Minimum people needed as collectors	1	1	1
How often the data is collected?	One session	One session	One session
Sample size: the number of data points collected per sample	1	1	1
When the data are collected?	TBD	TBD	TBD

The details for data collection plans are provided in Table H-14.

*Table H-14. Data collection plan for cucumber and frame distance, harvesting cycle and number of pods*

	Cucumber and frame distance	Harvesting cycle (growth rate)	Number of pods in each row
Definition	There is a horizontal metal frame above ground in greenhouse: For placing container under cucumbers, the container should be placed in that distance	The number of days that take to have ripened cucumbers	The number of pods in each row to find the speed of harvesting
How? Methods	Manual measurement	Interviewing	Observation
What instruments?	measuring tape	N/A	N/A
Why? Which research questions will be addressed?	Container design	For the date of real tests in farm	Robot performance

Sample frequency: How much/many data	Random 30 pods	N/A	N/A
Data type (continuous or discrete, quantitative or qualitative)	Discrete, quantitative	discrete, quantitative	discrete, quantitative
Data sources	Commercial greenhouses	Commercial greenhouses's people	Commercial greenhouses
Limitations	N/A	N/A	N/A
Predicted needed time (minutes)	60	20	20
Minimum people needed as collectors	1	1	1
How often the data is collected?	One session	One session	One session
Sample size: the number of data points collected per sample	2	N/A	N/A
When the data are collected?	TBD	TBD	TBD

### ***Appendix I. Boundary detection using ImageJ and Fiji***

Image processing for detection requires specialized platforms. ImageJ and Fiji, open-source programs, stand out for its versatility in handling various image formats. Offering a range of adjustments such as thresholding and brightness modification, they empower users to fine-tune visual data. After importing an image, analysis involves extracting specific information and measurements, utilizing pre-existing plugins, or creating custom ones for advanced tasks. In this study, segmentation and thresholding are performed initially, followed by utilization of some detection plugin to identify the borders and edges of plant components.

The results of applying colour threshold and some other filters, are shown in Figure 4-10. The system removed the background and focused on green colours. By utilizing the colour deconvolution option, quality of image processing is enhanced. Additionally, the edges are eroded to enhance the quality of connecting points and edges as shown in Figure 4-11. The only unresolved step in this part of study involves accurately keeping the boundaries of cucumbers while excluding the vines and leaves' boundaries. Future research will require detailed geometric analysis to differentiate between cucumber boundaries and those of the vines and leaves. Once this understanding of geometry is established, the cucumber's boundaries can be retained while the boundaries of vines and leaves are removed, facilitating cucumber detection.



*Figure I-1. Background removal*



*Figure I-2. The deconvolution option and finding the edges of plant components and final polish on edge detection using eroded option*



### ***Appendix J. Cucumber bounding box detection using Roboflow platform***

Like YOLO, first images are labeled in RoboFlow. After the training is completed, the model is tested with three images, and one sample is presented in Figure 4-12. The model also provides the position of each detected cucumber, along with its height, width, and confidence level.



*Figure J-1. The sample test used to see the accuracy of trained model*

## VITA AUCTORIS

NAME: Shahryar Ghorbanirezaei

PLACE OF BIRTH: Esfarayen, North Khorasan, IR

YEAR OF BIRTH: 1990

EDUCATION: Dr. Hesabi High School, Esfarayen, North Khorasan,  
IR, 2007

Babol Noshirvani University of Technology, B.Sc.,  
Babol, Mazandaran, IR, 2012

Tarbiat Modares University, Tehran, IR, 2015

University of Windsor, MAsc., Windsor, ON, 2024